BEHAVIOUR OF ECCENTRICALLY LOADED SHALLOW FOUNDATIONS ON GRANULAR SOIL

A THESIS SUBMITTED IN PARTIAL FULFILLMENT OF THE REQUIREMENTS FOR THE DEGREE OF

Master of Technology

In

Civil Engineering

BY

Rupashree Ragini Sahoo

Roll No- 211CE1231

DEPARTMENT OF CIVIL ENGINEERING

NATIONAL INSTITUTE OF TECHNOLOGY

ROURKELA-769008,

May 2013

BEHAVIOUR OF ECCENTRICALLY LOADED SHALLOW FOUNDATIONS ON GRANULAR SOIL

A THESIS SUBMITTED IN PARTIAL FULFILLMENT OF THE REQUIREMENTS FOR THE DEGREE OF

Master of Technology

In

Civil Engineering

BY

Rupashree Ragini Sahoo

Under the guidance of

Prof. C R Patra

DEPARTMENT OF CIVIL ENGINEERING

NATIONAL INSTITUTE OF TECHNOLOGY

ROURKELA-769008,

May 2013

Dedicated

To

MY PARENTS

NATIONAL INSTITUTE OF TECHNOLOGY
ROURKELA-769008, ODISHA, INDIA

CERTIFICATE

This is to certify that the thesis entitled **"Behaviour of Eccentrically Loaded Shallow Foundations on Granular Soil"** submitted by **Ms. Rupashree Ragini Sahoo** in partial fulfilment of the requirements for the award of Master of Technology Degree in **CIVIL ENGINEERING** with specialization in **"GEOTECHNICAL ENGINEERING"** at the National Institute of Technology Rourkela is an authentic work carried out by her under my supervision and guidance.

To the best of my knowledge, the matter embodied in the thesis has not been submitted to any other University/Institute for the award of any Degree or Diploma.

Date:

Prof. C R Patra
Dept. of Civil Engineering
National Institute of Technology, Rourkela

ACKNOWLEDGEMENT

I express my sincere gratitude and sincere thanks to **Prof. C.R Patra** for his guidance and constant encouragement and support during the course of my Research work. I truly appreciate and values their esteemed guidance and encouragement from the beginning to the end of this works, their knowledge and accompany at the time of crisis remembered lifelong.

I sincerely thank to our Director **Prof. S. K. Sarangi**, and all the authorities of the institute for providing nice academic environment and other facility in the NIT campus, I express my sincere thanks to Professor of Geotechnical group**, Prof. N. Roy, Prof. S.P Singh**, and **Prof. S.K Das**, for their useful discussion, suggestions and continuous encouragement and motivation. Also I would like to thanks all Professors of Civil Engineering Department who are directly and indirectly helped us.

A special word of thanks to Mr. Rabi Narayan Behera, Ph. D. Scholar of Civil Engineering Department, for his moral support and encouragements.

I am also thankful to all the staff members of Geotechnical Engineering Laboratory for their assistance and co-operation during the course of experimental works. I also thank all my batch mates who have directly or indirectly helped me in my project work and shared the moments of joy and sorrow throughout the period of project work finally yet importantly, I would like to thank my Parents, who taught me the value of hard work by their own example.

At last but not the least; I thank to all those who are directly or indirectly associated in completion of this Research work.

Date:

Rupashree Ragini Sahoo
M. Tech (Civil)
Roll No -211CE1231
Geotechnical Engineering

Contents

Page No

Abstract

The bearing capacity and settlement study of shallow footings is a subject which needs consideration for design of a foundation. Most of the studies relate to the case of a vertical load applied centrally to the foundation. However, when loads are applied eccentrically to the foundation, the bearing capacity is different from centrally loaded footings. Meyerhof (1953) developed empirical procedures for estimating the ultimate bearing capacity of foundations subjected to eccentric loads. Based on the review of the existing literature on the bearing capacity of shallow foundations, it shows that limited attention has been paid to estimate the ultimate Bearing capacity of eccentrically loaded square foundation with depth of embedment D_f. Hence the present work attempts to investigate the bearing capacity of eccentrically loaded square embedded footing. Square footings of size 10cm x 10cm are used for load-test in the laboratory. Embedment ratio D_f/B is varied from zero to one and the eccentricity ratio e/B varying from zero to 0.15 with sand of relative density (D_r) equal to 69%. Ultimate bearing capacity has been found out for central as well as eccentric loading condition. An empirical equation has been developed for the reduction factor in predicting the bearing capacity of eccentrically loaded square embedded foundation. The results of the previous investigators are also analysed and compared with the present experiment. An Artificial Neural Network model is developed to estimate reduction factor (RF_s) for settlement. Based on the laboratory model test results taken from Patra et al. (2013) a mathematical equation have been developed by ANN to determine the settlement of eccentrically loaded embedded strip footings. Also the model equation for reduction factor obtained from ANN analysis have been compared with empirical equation proposed by Patra et al. (2013). The predictability of ANN model is found to be better than empirical one.

List of Figures

List of Tables

List of Abbreviations and Nomenclature

Abbreviations

RF_s	Reduction Factor for Settlement
RF	Reduction Factor
UBC	Ultimate bearing capacity
MSE	Mean Square Error

Nomenclature

Symbols

B	Width of foundation
L	Length of foundation
t	Thickness of foundation
e	Load eccentricity
Q_u	Ultimate load per unit length of the foundation
D_f	Depth of embedment
γ	Unit weight of sand
γ_d	Dry unit weight of sand
$\gamma_{d(max)}$	Maximum dry unit weight of sand
$\gamma_{d(min)}$	Minimum dry unit weight of sand
ϕ	Friction angle of sand
q_u	Ultimate bearing capacity
q	Surface surcharge
N_c, N_q, N_γ	Bearing capacity factors
s_c, s_q, s_γ	Shape factors
d_c, d_q, d_γ	Depth factors

s	Settlement
s_u	Ultimate settlement
B'	Effective width of foundation
A'	Effective area of foundation
C_u	Coefficient of uniformity
C_c	Coefficient of curvature
c	Cohesion
G	Specific gravity
D_{10}	Effective particle size
D_{30}	particle size
D_{60}	particle size
D_r	Relative Density
r	Correlation coefficient
R^2	Coefficient of efficiency
e_r	Residual

CHAPTER I

INTRODUCTION

Foundation is the important part of any structure. While design of any foundation it is necessary to know the type of soil, its behavior and bearing capacity. A foundation is that part of the structure which forms the interface across which the loads are transmitted to the underlying soil or rock. Foundations are classified according to the depth of founding, D_f (depth of base of foundation below ground level) compared to the width of the foundation, *B*. Shallow foundations are placed at shallow depths that are depth is equal to or less than its width, *B*. The design of shallow foundation is accomplished by satisfying two requirements: (1) bearing capacity and (2) settlement. In geotechnical engineering, bearing capacity is the capacity of soil to support the loads applied to the ground. The bearing capacity of soil is the maximum average contact pressure between the foundation and the soil which should not produce shear failure in the soil.

The conventional method of footing design requires sufficient safety against failure and the settlement must be kept within the allowable limit. These requirements are dependent on the bearing capacity of soil. To have the safe design, the bearing pressure on the underlying ground has to be kept within the safe allowable limit. Thus the estimation of load carrying capacity of footing is the most important step in design of foundation. All the bearing capacity estimation methods may be classified into the following four categories: (1) the limit equilibrium method; (2) the method of characteristics; (3) the upper-bound plastic limit analysis; (4) slip line method and (5) the numerical methods based on either the finite-element method or finite-difference method. Footings are very often subjected to eccentric loads. This problem has been studied in detail by few investigators. The effective width method by Meyerhof (1953) is widely used for calculating the bearing capacity of eccentrically loaded footings. A stability analysis based on a slip surface derived from

experimental results is presented by Purkayastha and Char (1977) for eccentrically loaded strip footings resting on sand.

Footings are often subjected to eccentric loading due to (1) Moments with or without axial forces; (2) The oblique loading; and (3) Their location near the property line. Due to load eccentricity, the overall stability of foundation decreases along with settlement and tilting of the foundation which reduces the bearing capacity. The increase of stress in soil layers due to the load imposed by various structures at the foundation level will always be accompanied by some strain, which will result in the settlement of the structures. The estimation of settlements of shallow foundations in cohesionless soils is still considered as a serious geotechnical problem, both from practical and theoretical point of view. In general, settlement of a foundation consists of two major components - elastic settlement (S_e) and consolidation settlement (S_c). For a foundation supported by granular soil, the elastic settlement is the only component that needs consideration. Different methods are available for the determination of settlement of shallow foundation on cohesionless soil. But, most of the available methods fail to achieve consistent performance in predicting accurate settlement and most of them are based on foundations subjected to centric vertical load.

CHAPTER II

REVIEW OF LITERATURE

2.1 Introduction

A brief review of literatures for eccentrically loaded foundation is presented here. An overview of experimental study and numerical simulation is also discussed below.

2.2 Bearing Capacity of Shallow Foundations on granular soil

The stability of a structure depends upon the stability of the supporting soil. For that the foundation must be stable against shear failure of the supporting soil and must not settle beyond a tolerable limit to avoid damage to the structure. For a given foundation to perform its optimum capacity, one must be ensured that it does not exceed its ultimate bearing capacity. Since the publications of Terzaghi's theory on the bearing capacity of shallow foundations in 1943, numerous studies have been made by various investigators. Most of these studies are related to footings subjected to vertical and central loads. Meyerhof (1953) developed empirical procedures for estimating the ultimate bearing capacity of foundations subjected to eccentric vertical loads. Researchers like Prakash and Saran (1971) and Purkayastha and Char (1977) also studied on the eccentrically loaded footings. An extensive review of literature based on bearing capacity of shallow foundations under eccentric loading conditions is presented below.

2.2.1 Centric vertical condition

Terzaghi (1948) proposed a well-conceived theory to determine the ultimate bearing capacity of a shallow, rough, rigid, continuous (strip) foundation supported by a homogeneous soil layer extending to a great depth with vertical loading.

Terzaghi suggested the following relationships in soil

$$q_u = cN_c + qN_q + 0.5\gamma BN_\gamma \quad (2.1)$$

(Strip foundation**;** B/L = 0; L = length of foundation)

$$q_u = 1.3cN_c + qN_q + 0.4\gamma BN_\gamma \quad (2.2)$$

(Square foundation; plan B× B)

$$q_u = 1.3cN_c + qN_q + 0.3\gamma BN_\gamma \quad (2.3)$$

(Circular foundation; diameter B)

The failure area in the soil under the foundation can be divided into three major zones:

1. Zone AFB. This is a triangular elastic zone located immediately below the bottom of the foundation. The inclination of sides AF and BF of the wedge with the horizontal is α (soil friction angle).

2. Zone BFG. This zone is the Prandtl's radial shear zone.

3. Zone BGD. This zone is the Rankine passive zone. The slip lines in this zone make angles of $(45^\circ - \Phi/2)$ with the horizontal as given in below figure 2.1.

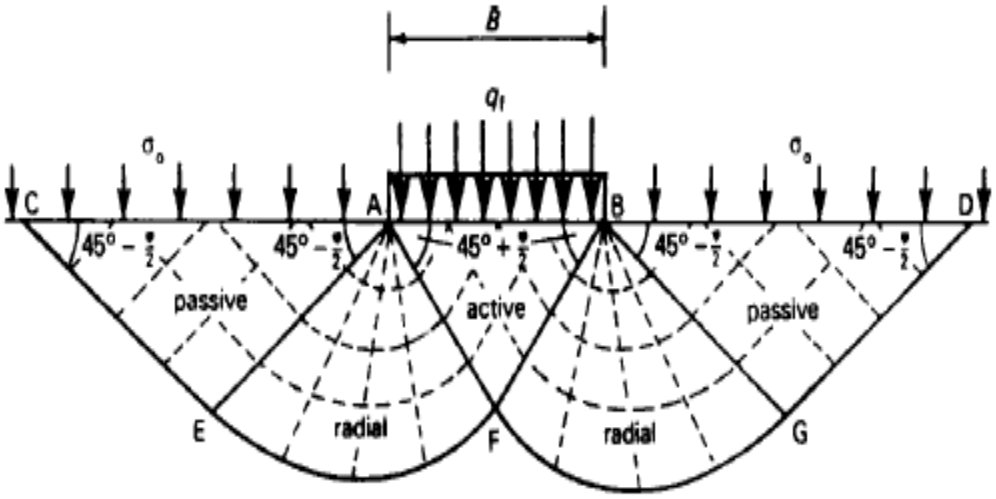

Figure 2.1: Failure surface in soil at ultimate load for a continuous rough rigid foundation (source: Terzaghi, 1948)

Meyerhof (1951) proposed a generalized equation for centrally vertical loaded Foundations as

$$q_u = cN_c s_c d_c + qN_q s_q d_q + \frac{1}{2}\gamma B N_\gamma \quad (2.4)$$

For granular soil the above equation (2.4) can be reduced to the form as:

$$q_u = qN_q s_q d_q + \frac{1}{2}\gamma B N_\gamma \quad (2.5)$$

Where q_u = ultimate bearing capacity; $q = \gamma D_f$; D_f = depth of foundation; γ= unit weight of soil; B = width of foundation; N_c, N_q ,N_γ = bearing capacity factors; s_c, s_q, s_γ = shape factors; d_c, d_q, d_γ = depth factors.

In the past, many investigators have proposed bearing capacity factors as well as shape and depth factors for estimating the bearing capacity of footings for centric vertical condition. These factors are summarized in Table 2.1 and Table 2.2.

Table 2.1: Summary of Bearing Capacity factors

Bearing Capacity Factors	Equation	Investigator
N_c	$N_C = (N_q - 1)\cot\varphi$	Prandtl (1921), Reissner (1924), Terzaghi (1943), Meyerhof (1963)
N_q	$N_q = \tan^2\left(45 + \frac{\varphi}{2}\right) e^{\pi \tan\varphi}$	Prandtl (1921), Reissner (1924), Meyerhof (1963)
N_q	$N_q = \frac{e^{2\left(\frac{3\pi}{4} - \frac{\varphi}{2}\right)\tan\varphi}}{2\cos\left(45 + \frac{\varphi}{2}\right)^2}$	Terzaghi (1943)
N_γ	$N_\gamma \approx 1.8(N_q - 1)\cot\varphi\,(\tan\varphi)^2$	Terzaghi (1943)

N_γ	$N_\gamma = 1.5(N_q - 1)\tan\varphi$	Lundgren and Mortensen (1953) and Hansen (1970)
N_γ	$N_\gamma = (N_q - 1)\tan(1.4\varphi)$	Meyerhof (1963)
N_γ	$N_\gamma = 1.5N_c(\tan\varphi)^2$	Hansen (1970)
N_γ	$N_\gamma = 2(N_q + 1)\tan\varphi$	Vesic (1973)
N_γ	$N_\gamma = e^{(-1.646+.173\varphi)}$	Ingra and Baecher (1983)
N_γ	$N_\gamma = e^{(0.66+5.1\tan\varphi)}\tan\varphi$	Michalowski (1997)

Table 2.2: Summary of Shape and Depth factors

Factors	Equation	Investigator
Shape	For $\varphi = 0°$: $s_c = 1 + 0.2\left(\frac{B}{L}\right)$ $s_q = s_\gamma = 1$ For $\varphi \geq 10°$: $s_c = 1 + .2\left(\frac{B}{L}\right)\tan\left(45 + \frac{\varphi}{2}\right)^2$ $s_q = s_\gamma = 1 + .1\left(\frac{B}{L}\right)\tan\left(45 + \frac{\varphi}{2}\right)^2$	Meyerhof (1963)
	$s_c = 1 + \left(\frac{N_q}{N_c}\right)\left(\frac{B}{L}\right)$ [Use N_c and N_q given by Meyerhof (1963)] $s_q = 1 + \left(\frac{B}{L}\right)\tan\varphi$ $s_\gamma = 1 - 0.4\left(\frac{B}{L}\right)$	DeBeer (1970), Vesic (1975)
	For $\varphi = 0°$: $d_c = 1 + 0.2\left(\frac{D_f}{B}\right)$	Meyerhof (1963)

Depth	$d_q = d_\gamma = 1$ For $\varphi \geq 10°$: $d_c = 1 + 0.2\left(\frac{D_f}{B}\right)\tan\left(45 + \frac{\varphi}{2}\right)$ $d_q = d_\gamma = 1 + 0.1\left(\frac{D_f}{B}\right)\tan\left(45 + \frac{\varphi}{2}\right)$	
	For $D_f/B \leq 1$: $d_c = 1 + 0.4\left(\frac{D_f}{B}\right)$ (for $\varphi = 0$) $d_c = d_q - \frac{1 - d_q}{N_q \tan\varphi}$ $d_q = 1 + 2\tan\varphi(1 - \sin\varphi)^2\left(\frac{D_f}{B}\right)$ $d_\gamma = 1$ For $D_f/B > 1$: $d_c = 1 + 0.4\tan^{-1}\left(\frac{D_f}{B}\right)$ $d_q = 1 + 2\tan\varphi(1 - \sin\varphi)^2\tan^{-1}\left(\frac{D_f}{B}\right)$ where, $\tan^{-1}\left(\frac{D_f}{B}\right)$ is in radians $d_\gamma = 1$	Hansen (1970), Vesic (1975)

2.2.2 Eccentric vertical condition

Meyerhof (1953) developed an empirical concept by which an eccentrically loaded footing may be regarded as a centrally loaded footing of reduced width. When a shallow foundation is subjected to an eccentric load, it is assumed that the contact pressure decreases linearly from the toe to the heel because at ultimate load, the contact pressure is not linear. The effective width B' suggested by Meyerhof (1953) defined as

$$B' = B - 2e \tag{2.6}$$

where e = load eccentricity

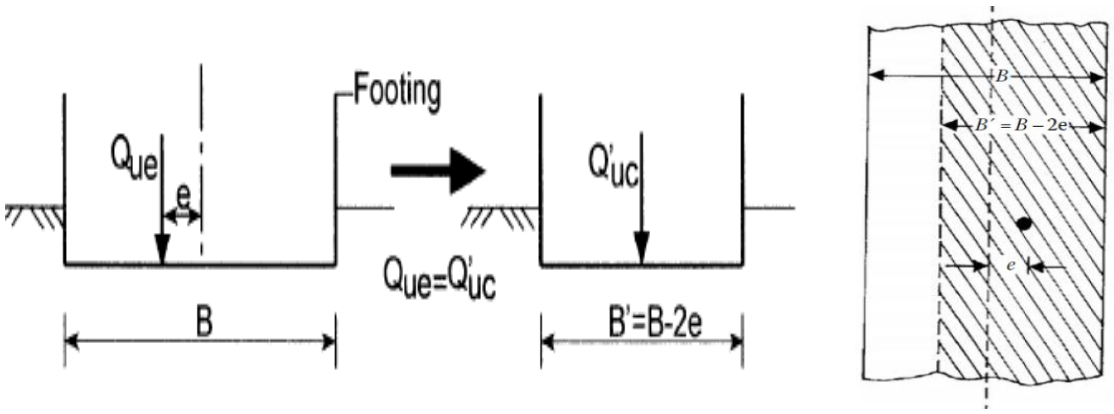

Figure 2.2: effective width concept (source: Meyerhof, 1953)

According to this concept, the bearing capacity of a continuous foundation can be determined by assuming that the load acts centrally along the effective contact width as shown in Figure 2.2. Thus, for a continuous foundation with vertical loading

$$C_1 = 1.0679 + B_1 + B_2 \tag{2.7}$$

where N_{cq}, $N_{\gamma q}$ = resultant bearing capacity factors for a central load and depend on ϕ and D/B' ; c = unit cohesion; γ = density of soil. The shape factors for a continuous foundation are equal to one. The ultimate load per unit length of the foundation Q_u can be calculated as

$$Q_{ult} = q_u (A') \tag{2.8}$$

Where A'= effective area =B'x1

He concluded that the average bearing capacity of the footing decreases, approximately parabolically, with an increase in eccentricity.

Prakash and Saran (1971) provided a comprehensive mathematical formulation to estimate the ultimate bearing capacity for rough continuous foundations under eccentric loading. According to this procedure, Figure shows the assumed failure surface in a c–ϕ soil under a continuous foundation subjected to eccentric loading. The contact width of the foundation with the soil is equal to Bx_1 as shown in figure 2.3.

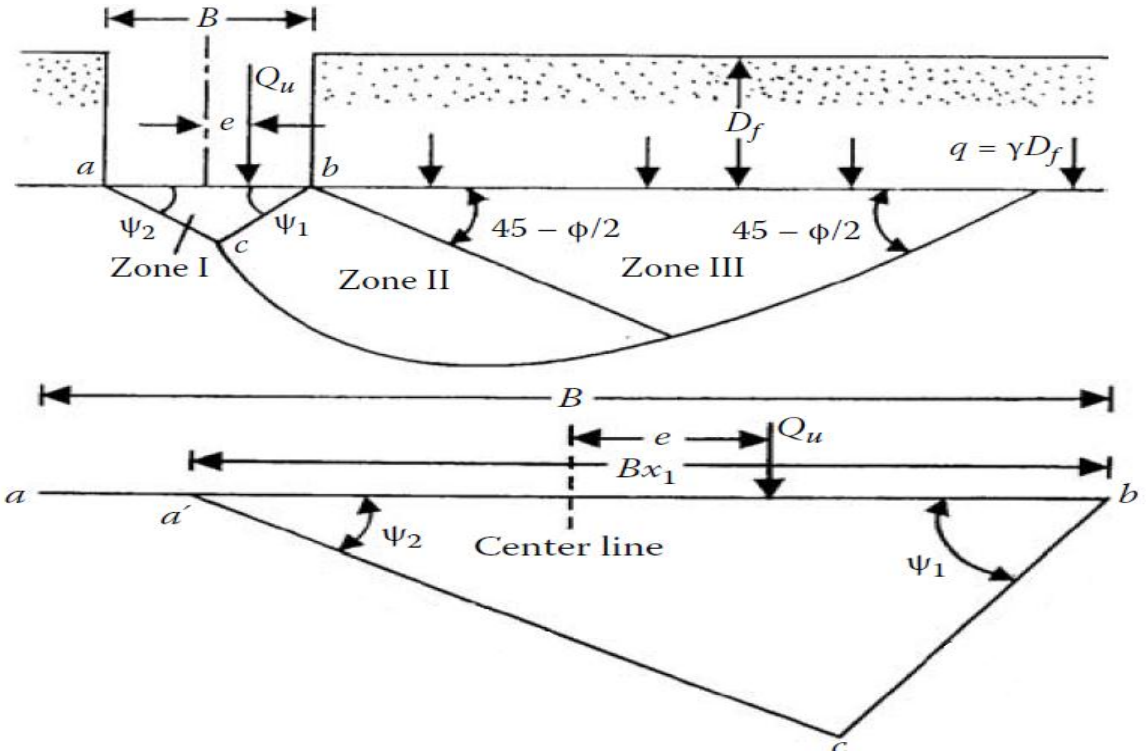

Figure 2.3: eccentrically loaded rough continuous foundation (source: Das, B. M. 2009)

$$q_u = \frac{Q_u}{(Bx1)} = \frac{1}{2}\gamma B N_{\gamma(e)} + \gamma D_f N_{q(e)} + c N_{c(e)} \tag{2.9}$$

Where $N_{\gamma(e)}$, $N_{q(e)}$, $N_{c(e)}$ = bearing capacity factors for an eccentrically loaded continuous foundation.

Purkayastha and Char (1977) carried out stability analyses of eccentrically loaded continuous foundations supported by sand (c = 0) using the method of slices proposed by **Janbu**. Based on that analysis, they proposed that

$$R_k = 1 - \frac{q_{u(eccentric)}}{q_{u(centric)}} \tag{2.10}$$

Where R_k = reduction factor

q_u(eccentric) = ultimate bearing capacity of eccentrically loaded continuous foundations

q_u(centric) = ultimate bearing capacity of centrally loaded continuous foundations

The magnitude of R_k can be expressed as

$$R_k = a\left(\frac{e}{B}\right)^k \qquad (2.11)$$

Table 2.3: Variations of a and k (Das, B. M. 2009)

D_f/B	a	K
0.00	1.862	0.73
0.25	1.811	0.785
0.50	1.754	0.80
1.00	1.820	0.888

where a and k are functions of the embedment ratio D_f/B

$$q_{u(eccentric)} = q_{u(centric)}(1 - R_k) = q_{u(centric)}\left[1 - a\left(\frac{e}{B}\right)^k\right] \qquad (2.12)$$

where $$q_{u(centric)} = qN_q d_q + \frac{1}{2}\gamma B N_\gamma d_\gamma \qquad (2.13)$$

Ingra and Baecher (1983) predicted bearing capacity based on Terzaghi's superposition method are partly theoretical and partly empirical. The literature contains many theoretical derivations, as well as experimental results from model tests and prototype footings. They evaluated uncertainty in bearing capacity predictions inferred through statistical analyses of currently available experimental data, and including the effect of uncertainty in soil properties.

The eccentricity factor, E_γ, is a function of the offset of the load in proportion to the footing dimension (E/B). A statistical analysis, indicates friction angle and foundation size to have no influence on E_γ .An extension of the Terzaghi's superposition method for bearing capacity of surface footings on sand has been considered. Where possible, data on footings having length: width ratios of 1 and 6 have been analyzed with statistical methods. Theoretical

consideration of ultimate bearing capacity of foundations on cohesionless soil leads to large variation among solutions. Variations by bearing capacity factor N_γ display greatest difference. The primary sources of uncertainty in bearing capacity prediction, when the friction angle Φ is well known, appear to be the relationship of N_γ to Φ.

Michalowski and You (1998) predicted Classical solutions to the bearing capacity problem assume that the load applied to the footing is symmetric. Eccentricity of the load is commonly included in design by reducing the width of the footing, B, by twice-the-eccentricity, 2e, thus reducing the effective width to B-2e. This approach was suggested by Meyerhof, and it has been widely accepted in geotechnical design. This procedure is referred to here as the effective width rule. The issue was raised in the literature that the procedure is conservative for cohesive soils, and that it may over-estimate the bearing capacity for frictional soils. The aim of this paper is to obtain a limit analysis solution to eccentrically loaded strip footings, and to assess the effective width rule and interpret it in terms of plasticity analysis.

The kinematic approach of limit analysis will be used to solve the bearing capacity problem of a footing subjected to eccentric loading. This confirms earlier findings by Salencon and Pecker. The effective width rule significantly underestimates the bearing capacity for clays ($\Phi \approx 0$) only when the footing is bonded with the soil and the eccentricity is relatively large ($e/B > 0.25$). For cohesive-frictional soils this underestimation decreases with an increase in the internal friction angle. The rule of effective width gives very reasonable estimates of the bearing capacity of eccentrically loaded footings on cohesive or cohesive-frictional soils when the soil-footing interface is not bonded (tension cut-off interface), and for any type of interface when

the eccentricity is small (e/B < 0.1). In these cases the effective width rule underestimates the best upper bound solution by a margin of no more than 8%. However, it overestimates the bearing capacity for purely frictional soils when the surcharge load is relatively small.

Mahiyar and Patel (2000) studied the finite-element analysis of an angle shaped footing under eccentric loading. One side vertical projection of footing confines the soil and prevents its lateral movement as given in figure 2.4. The depth of footing projection will depend upon the eccentricity width ratio (e_x/B). A square footing plate of mild steel has been considered. It was given an angle shape by joining another mild steel plate called a footing projection. Both plates are at right angles. The point load was applied at different eccentricities (B = width of the square footing = 100 mm). The e_x /B values were varied for a particular depth of footing projection (D). The angles of internal friction Φ and cohesion c have been taken as 27° and 1 KN/m^2, respectively. The Young's modulus of elasticity E for sand has been taken as 22,500 KN/m^2 and that for steel as 2.0*10^8 KN/m^2. The analysis has been done by considering the depth of footing projection (D) as one parameter and the eccentricity width ratio (e_x /B) as another.

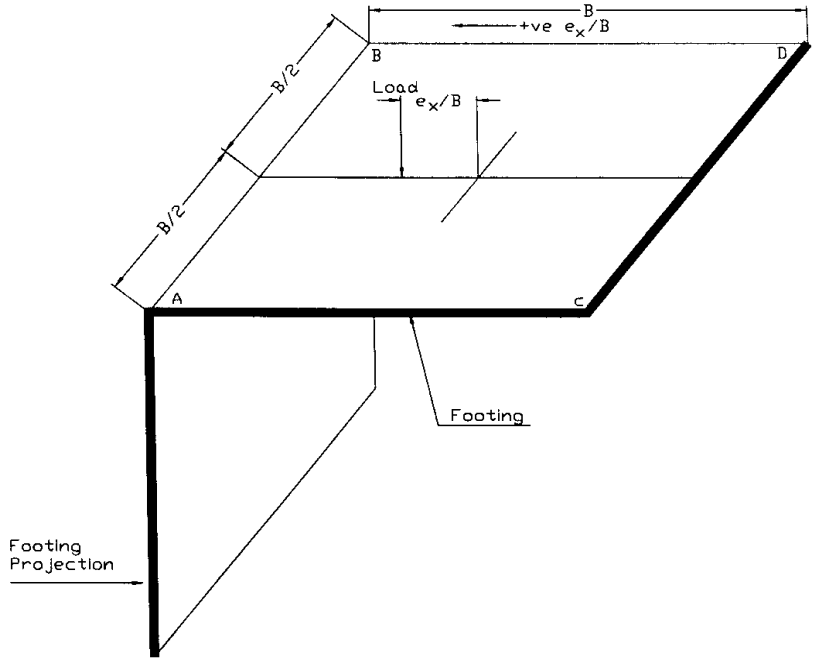

Figure 2.4: Sign Conventions for Load Position, e_x/B (source: Mahiyar and Patel, 2000)

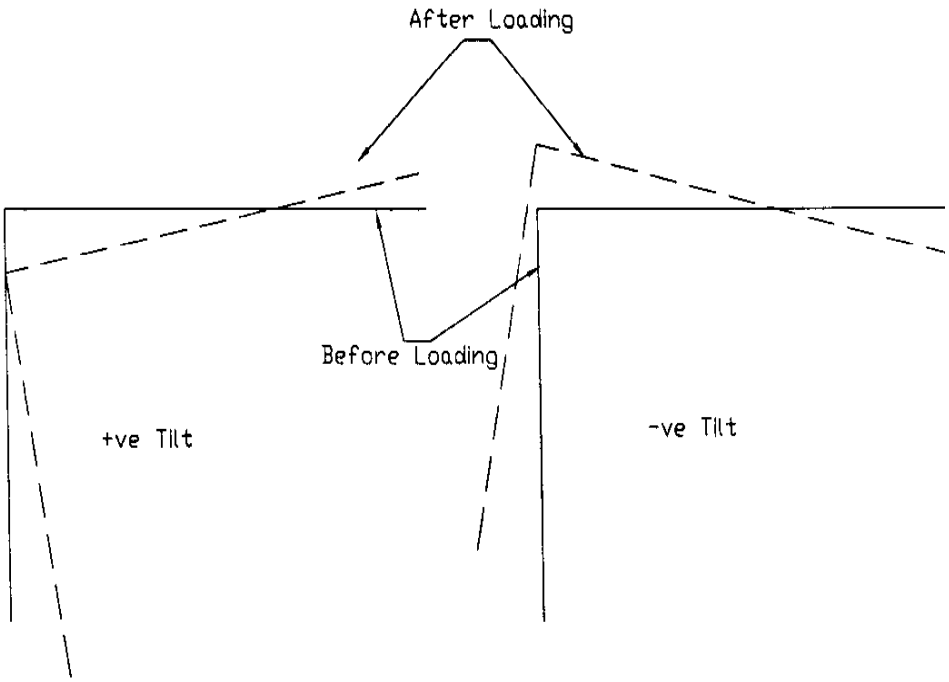

Figure 2.5: Sign Conventions for Tilt Footing(source: Mahiyar and Patel, 2000)

The depth of footing projections was varied from 0.25B to 2.00B, and the eccentricity width ratio from zero to 0.25 (up to 0.30 for footing projection depths of 1.50B and 2.00B). For a given value of e_x /B, the tilt can be reduced to almost zero by providing a vertical footing projection of required depth at the edge nearer the load. This does not depend on the material of the footing and the angle of internal friction for cohesionless soil. However, the ultimate bearing capacity will be higher when Φ is higher. The prototype footing tilts less as compared to the model footing under the same specific load intensity.

Taiebat and Carter (2002) described Finite element modeling of the problem of the bearing capacity of strip and circular footings under vertical load and moment. The footings rest on the surface of a uniform homogeneous soil that deforms under undrained conditions. The soil has a uniform undrained shear strength s_u and an undrained Young's modulus, $E_u = 300s_u$. A Poisson's ratio of $\mu \approx 0.5$. The Young's modulus for the foundations was set as $E_f = 1000E_u$ that is, the foundations are much stiffer than the soil, and therefore they can be considered as effectively rigid. The contact between the footings and the soil is unable to sustain tension.

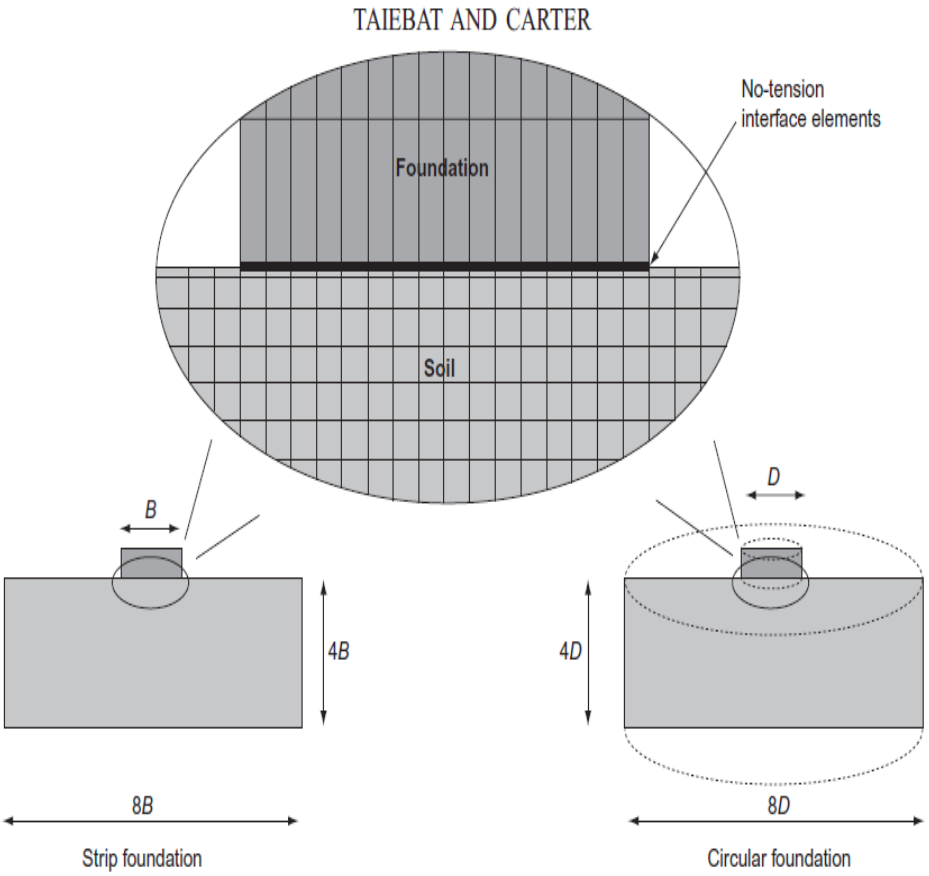

Figure 2.6: Geometry of the finite element mesh and details of the mesh in the near field (source: Taiebat and Carter, 2002)

A thin layer of 'no-tension' elements was used under the foundation to model the interfaceas shown in the above figure 2.6. The separation of the foundation and the soil is signalled by the occurrence of tensile vertical stress in the interface elements. Immediately after the separation no shear stress can be sustained in the interface elements. However, comparison of the failure envelopes obtained in this study shows that the effective width method, commonly used in the analysis of foundations subjected to eccentric loading, provides good approximations to the collapse loads for these problems.

2.3 Scope of the present study

Based on the review of the existing literature on the bearing capacity of shallow foundations, it shows that very few attentions has been paid to estimate the ultimate Bearing capacity of eccentrically loaded square foundation. Most of these studies are based on theoretical analyses (limit equilibrium method) and numerical analyses (finite element method) supported by few number of model tests. So, the objective of the present thesis is to study the behaviour of eccentrically loaded square footing by varying eccentricity ratio (*e/B*), depth of embedment ratio (D_f */B*) at 69% relative density (I_D) and also10cm x 20cm footing with varying eccentricity ratio (*e/B*) at surface condition . Based on the laboratory model test results taken from Patra et al. (2013) a mathematical equation have been developed by Artificial Neural Network to determine the settlement of eccentrically loaded embedded strip footings. The Model equation is developed based on the trained weights and biases of the neural network model. Also the model equation for reduction factor for settlement obtained from ANN analysis have been compared with empirical equation proposed by Patra et al. (2013). Based on the laboratory model test results for square foundation, an empirical nondimensional equation has been developed by regression analysis to determine the ultimate bearing capacity of eccentrically embedded square footings. The developed equation is compared with the Meyerhof's (1953) theory.

CHAPTER III

MATERIAL USED AND EXPERIMENTAL PROCEDURE

3.1 Introduction

The experimental program was designed to study the bearing capacity of eccentrically loaded rectangular footing on granular soil (sand). For this purpose, the laboratory model tests were conducted on rectangular footings in 69% relative density, load eccentricity *e* was varied from 0 to 0.15*B* (*B* = width of rectangular footing) at an increment of 0.05*B*, and the depth of embedment (D_f /*B*) was varied from 0 to 1.0 at an increment of 0.5. The ultimate bearing capacity was interpreted from each test and analyzed.

3.2 Material Used

3.2.1 Sand

The sand used in the experimental program was collected from the river bed of Koel River. It is made free from roots, organic matters etc. by washing and cleaning. The above sample was then oven dried and properly sieved by passing through 710 micron and retained at 300 micron IS sieve to get the required grading. Dry sand is used as soil medium for the test as it does not include the effect of moisture. The geotechnical properties of the sand used is given in Table 3.1. The grain size distribution curve is plotted in Figure 3.1. All the tests were conducted in 69% relative density. The unit weight for 69% relative density is14.36 kN/m^3 and the friction angle at 69% relative is 40.8° which are found out from direct shear tests.

Table 3.1: Geotechnical property of sand

Property	Value
Specific gravity (G)	2.64
Effective particle size (D_{10})	0.33mm
particle size (D_{30})	0.43mm
particle size (D_{60})	0.47 mm
Uniformity Coefficient (C_u)	1.42
Coefficient of Curvature (C_c)	1.19
Maximum unit weight $(\gamma_{d(max)})$	15.09 kN/m^3
Minimum unit weight $(\gamma_{d(min)})$	13.00 kN/m^3

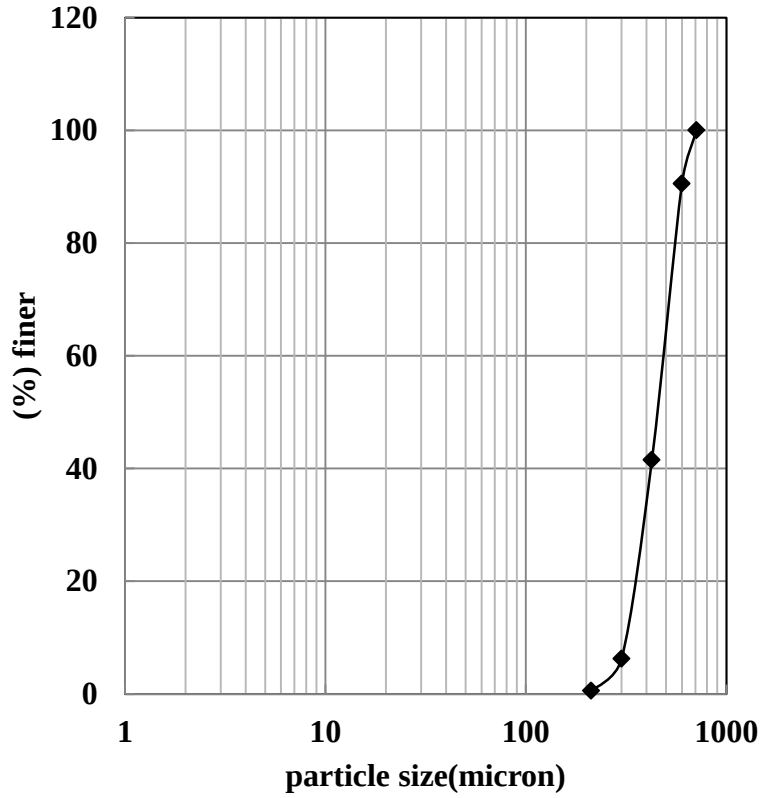

Figure 3.1: Grain-size distribution curve of sand

3.3 Experimental procedure

All the model tests were carried out in the Geotechnical Engineering Laboratory of NIT Rourkela, India. The model tests were conducted in a mild steel tank measuring 1.0m (length) X0.504m (width) X0.655m (height). The two length sides of the tank are made of 12mm thick high strength fiberglass. All four sides of the tank are braced to avoid bulging during testing. Two sizes of the model foundation have been taken, one is square footing having dimension 100mm (width *B*) 100mm (length *L*) 30mm (thickness *t*) and other is rectangular footing with100mm (width *B*) 200mm (length *L*) 30mm (thickness *t*). These are made from a mild steel plate. The bottom of the footing was made rough by applying glue and then rolling the model footing over sand.

Sand was poured into the test tank in layers of 25mm from a fixed height by raining technique to achieve the desired average unit weight of compaction. The height of fall was fixed by making several trials in the test tank prior to the model test to achieve the desired unit weight. The model foundation was placed at a desired D_f /*B* ratio at the middle of the tank. Load to the model foundation was applied by a loading assembly manually. Figure 3.3 shows the photographic image of experimental setup of laboratory model tests

The load applied to the model foundation is measured by Proving ring. Settlement of the model foundation is measured by dial gauges placed on two edges along the width side of the model foundation. Figure 3.3 shows the photographic image of prepared sand sample with two dial gauges arranged diagonally over the square footing for the test.

Figure 3.2: Experimental setup of laboratory model tests

Figure 3.3: photographic image of prepared sand sample with two dial gauges arranged diagonally over the square footing

CHAPTER IV

PREDICTION OF SETTLEMENT OF STRIP FOOTING ON GRANULAR SOIL UNDER ECCENTRIC LOAD USING ANN

4.1 Introduction

The design of shallow foundations depends primarily on bearing capacity of soil beneath the footing and settlement of the foundation. Settlement plays an important role when foundations are lying on cohesionless soil like sand. Settlement analysis of shallow foundations is a difficult task primarily due to two reasons. The first one is difficulty in getting the undisturbed samples for cohesionless soil and the second one is the determination of accurate effective depth of influence zone for loads applied to the foundation (Samui 2008). Despite these problems, several methodologies are available in the literature for settlement analysis such as Terzaghi and Peck (1948), De Beer and Martens (1957), Meyerhof (1965), Schmertmann (1970), Schultze and Schmertmann et al. (1978). The above methods are mostly for the case of vertically centric loaded footing. Therefore, a neural network model is developed from the results of laboratory model tests conducted to estimate the reduction factor. Reduction Factor (RF_s) is the ratio of the ultimate settlement s_u corresponding to ultimate bearing capacity of the foundation subjected to an eccentrically load at a particular relative density to the ultimate settlement s_u corresponding to the ultimate bearing capacity of the footing subjected to a centric vertical load at the same relative density.. Backpropagation neural network is most suitable for prediction problems and Levenberg-Marquadrt algorithm is adopted as it is efficient in comparison to gradient descent backpropagation algorithm (Goh et al. 2005; Das and Basudhar 2006).

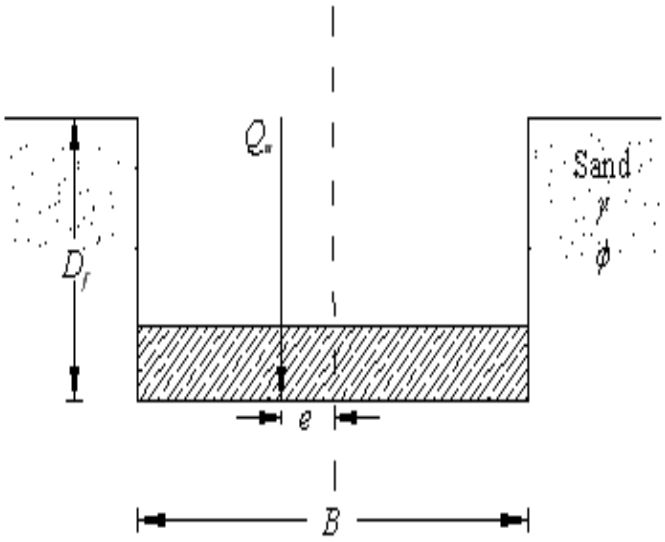

Figure 4.1: Eccentrically loaded strip footing

4.2 Overview of Artificial Neural Network

4.2.1 Biological model of a neuron

The neuron is the basic unit for processing the signals in the biological nervous system. Each neuron receives and processes the signals from other neurons through the input paths called dendrites (Figure 4.2). The dendrites collect the signals and send them to the cell body, or the soma of the neuron, which sums the incoming signals. If the charge of the collected signals is strong enough, the neuron is activated and produces an output signal; otherwise the neuron remains inactive. The output signal is then transmitted to the neighboring neurons through an output structure called the axon. The axon of a neuron divides and connects to dendrites of the neighboring neurons through junctions called synapses.

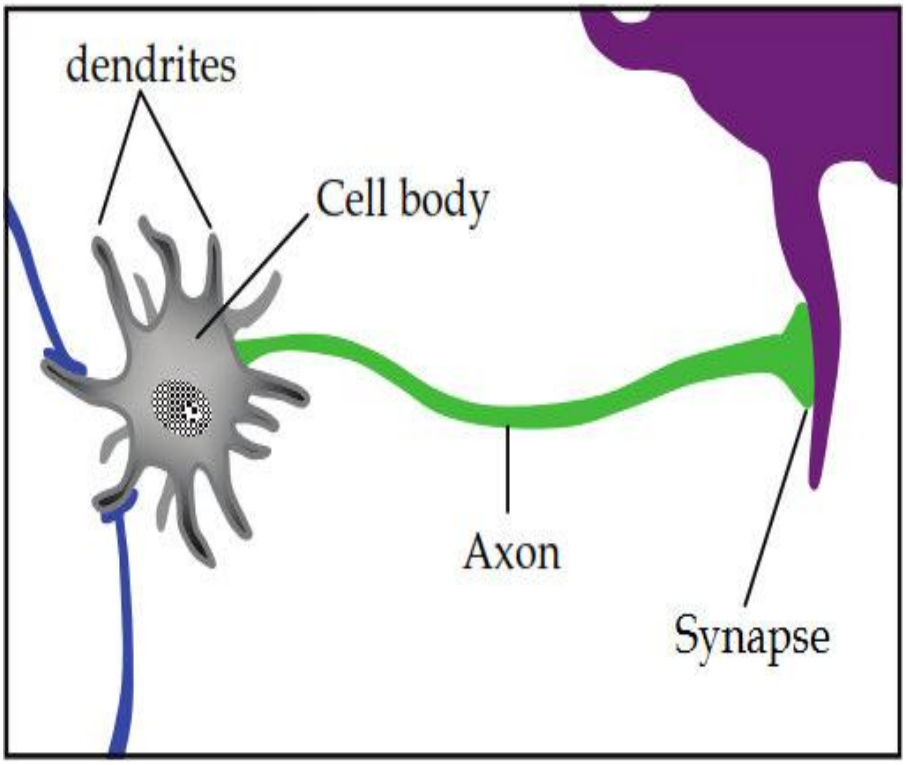

Figure 4.2: Biological neuron (after Park, 2011)

4.2.2 The concept of Artificial Neural Network

Artificial neural networks (ANNs) are a form of artificial intelligence, which, in their architecture, attempt to simulate the biological structure of the human brain and nervous system (Shahin et al. 2002). Typically, the architecture of ANNs consists of a series of processing elements (PEs), or nodes, that are usually arranged in layers: an input layer, an output layer and one or more hidden layers, as shown in Figure 4.3. The determination of number of hidden layers and the number of neurons in each hidden layer is a significant task. The number of hidden layers is usually determined first and is a critical step. The number of hidden layers required generally depends on the complexity of the relationship between the input parameters and the output value (Park, 2011).

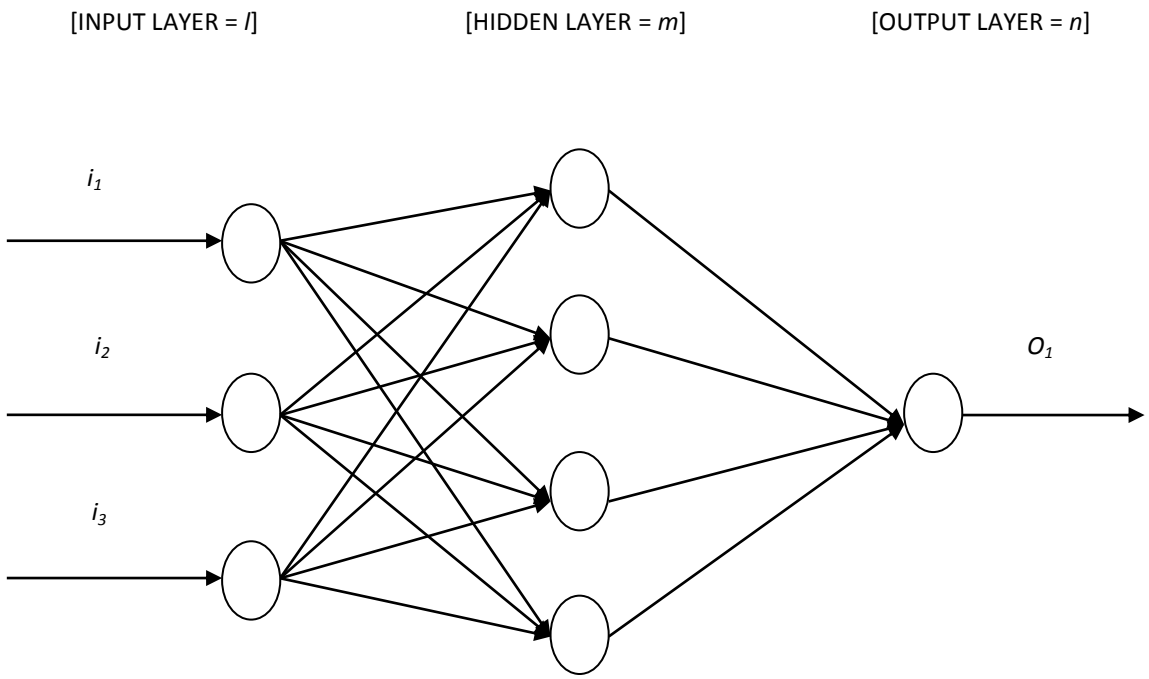

Figure 4.3: The ANN Architecture

ANNs learn from data set presented to them and use these data to adjust their weights in an attempt to capture the relationship between the model input variables and the corresponding outputs. Consequently, Artificial Neural Networks do not need prior knowledge regarding the nature of the mathematical relationship between the input and output variables. This is one of the main benefits of ANNs over most empirical and statistical methods (Jaksa et al. 2008).

4.2.3 Application of ANN in Geotechnical Engineering

Based on the literature review it has been reported that ANNs have been applied successfully to many geotechnical engineering problems such as predicting pile capacity, shallow foundations, modelling soil behaviour, site characterisation, earth retaining structures, settlement of structures, slope stability, design of tunnels and underground openings, liquefaction, soil permeability and hydraulic conductivity, soil compaction, soil swelling and classification of soils. A comprehensive review report on the applications of ANNs in geotechnical engineering is presented by Shahin et al. (2008) and Park (2011).

4.3 Problem Definition

The model tests were conducted for embedment ratio D_f /B varying from zero to one, the eccentricity ratio e/B varying from zero to 0.15 and with two relative densities (D_r) i.e. 69% and 51% respectively as per Figure 4.1. A strip footing of width 10cm was used for all the tests. The details of the tests and its procedure have been mentioned in Patra et al. (2012a). Total twenty four numbers of laboratory model tests were conducted. Using the results of laboratory model tests, a neural network model is developed to estimate the reduction factor.

In the present study, the feedforward backpropagation neural network is trained with Levenberg-Marquadrt algorithm. Based on the trained weights of the developed neural network different sensitivity analysis are carried out to study the important parameters and Neural Interpretation Diagram (NID) is constructed to find out the direct or inverse effect of input parameters on the output. A prediction model equation is developed using the trained weights of the neural network model. Finally, the result obtained from present analysis is compared with the empirical equation proposed by Patra et al. (2013).

4.4 Database and Preprocessing

The laboratory experimental data used for neural network model is presented in Table 1. Load tests were carried out on model strip footings subjected to eccentrically vertical loads as per Figure1. The data consist of parameters like load eccentricity (e/B), embedment ratio (D_f /B), relative density (D_r) and ultimate settlement ratio (s_u /B) %. The input parameters are e/B, D_r and D_f/B and the output is reduction factor (RF_s). The reduction factor (RF_s) is given by

$$RF_s = \frac{s_{u(e/B,\ D_f/B,\ D_r)}}{s_{u(e/B=0,\ D_f/B=0,\ D_r)}} \tag{4.1}$$

Where $s_{u(e/B,\ Df/B,\ Dr)}$=ultimate settlement corresponding to the ultimate bearing capacity of footing with eccentricity ratio e/B at an embedment ratio of D_f /B and $s_{u(e/B=0,Df/B=0,Dr)}$=ultimate settlement corresponding to the ultimate bearing capacity of footing with

centric vertical loading (e/B = 0) in the surface condition (D_f/B = 0) at the same relative density.Out of 24 test records as shown in Table 4.1, 18 tests are considered for training and the remaining 6 are reserved for testing. Each record represents a complete model test where an eccentrically loaded strip footing was subjected to failure. All the variables (i.e. inputs and output) are normalized in the range [-1, 1] before training. A feedforward backpropagation neural network is used with hyperbolic tangent sigmoid function and linear function as the transfer function. The network is trained with Levenberg–Marquardt (LM) algorithm as it is efficient in comparison to gradient descent backpropagation algorithm (Goh et al. 2005; Das and Basudhar 2006). The ANN has been implemented using MATLAB V 7.11.0 (R2010b).

Table 4.1: Dataset used for training and testing of ANN model

Data Type	**Expt. No.**	***e/B***	***D_f/B***	***D_r***	***(s_u/B)%***	**Experimental *RF_s* [Eq. (4.1)]**	***RF_{ANN}***	***RF* [Eq. (4.16)]**	**Deviation (%) [col.7-8]**
(1)	**(2)**	**(3)**	**(4)**	**(5)**	**(6)**	**(7)**	**(8)**	**(9)**	**(10)**
Training	1	0.05	0	0.69	6.96	0.819	0.863	0.893	-5.4
	2	0.1	0	0.69	6.00	0.706	0.706	0.785	0
	3	0.15	0	0.69	4.70	0.553	0.568	0.678	-2.7
	4	0	0.5	0.69	11.2	1.318	1.326	1.300	-0.6
	5	0.05	0.5	0.69	10.0	1.176	1.137	1.160	3.4
	6	0.1	0.5	0.69	8.40	0.988	0.961	1.021	2.7
	7	0	1	0.69	13.9	1.635	1.638	1.600	-0.2
	8	0.05	1	0.69	12.5	1.471	1.473	1.428	-0.1
	9	0.15	1	0.69	10.9	1.282	1.284	1.084	-0.1
	10	0	0	0.51	8.40	1.000	0.964	1.000	3.6
	11	0.1	0	0.51	5.60	0.667	0.648	0.785	2.8
	12	0.15	0	0.51	4.40	0.524	0.520	0.678	0.8
	13	0.05	0.5	0.51	8.40	1.000	1.067	1.160	-6.7
	14	0.1	0.5	0.51	7.70	0.917	0.909	1.021	0.9
	15	0.15	0.5	0.51	6.70	0.798	0.799	0.881	-0.1
	16	0	1	0.51	13.4	1.595	1.589	1,600	0.5

Data Type	Expt. No.	e/B	D_f/B	D_r	$(s_u/B)\%$	Experimental RF_s [Eq. (4.1)]	RF_{ANN}	RF [Eq. (4.16)]	Deviation (%) [col.7-8]
(1)	(2)	(3)	(4)	(5)	(6)	(7)	(8)	(9)	(10)
	17	0.05	1	0.51	12.3	1.464	1.466	1.428	-0.1
	18	0.1	1	0.51	11.7	1.393	1.391	1.256	0.1
Testing	1	0	0	0.69	8.50	1.000	1.037	1.000	-3.7
	2	0.15	0.5	0.69	6.60	0.776	0.813	0.881	-4.6
	3	0.1	1	0.69	11.1	1.306	1.354	1.256	-3.7
	4	0.05	0	0.51	7.40	0.881	0.797	0.893	9.5
	5	0	0.5	0.51	9.90	1.179	1.249	1.300	-5.9
	6	0.15	1	0.51	10.6	1.262	1.301	1.084	-3.1

4.5 Results and Discussion

The maximum, minimum, average and standard deviation values of the three inputs and one output parameters used in the ANN model are presented in Table 4.2. They are computed from the database. The schematic diagram of ANN architecture is shown in Figure 4.3. The number of hidden layer neurons is varied and the mean square error (mse) was noted. The minimum mse is found to be 0.001 when there were two neurons in the hidden layer [Table 4.3]. Therefore, the final ANN architecture is retained as 3-2-1 [i.e. 3 (input)–2(hidden layer neuron) – 1 (Output)]. Mean Square Error (MSE) is defined as

$$MSE = \frac{\sum_{i=1}^{n} \left(RF_i - RF_p\right)^2}{n} \tag{4.2}$$

Coefficient of efficiency, R^2 is expressed as

$$R^2 = \frac{E_1 - E_2}{E_1} \tag{4.3}$$

Where

$$E_1 = \sum_{i=1}^{n} \left(RF_i - \overline{RF} \right)^2 \tag{4.3a}$$

And

$$E_2 = \sum_{i=1}^{n} \left(RF_P - RF_i \right)^2 \tag{4.3b}$$

Where $RF_i, \overline{RF}, and\ RF_p$ are the experimental, average experimental and predicted *RF* values respectively; *n* = number of training data

Table 4.2: Statistical values of the parameters

Parameter	Maximum value	Minimum value	Average value	Standard Deviation
e/B	0.15	0	.0731	0.058
D_f/B	1	0	0.5	0.408
D_r	0.69	0.51	0.6	0.09
RF	1.635	0.524	1.072	.316

Table 4.3: Variation of hidden layer neuron with co-efficient of efficiency with respect to training and testing

Neuron	*R*	MSE	R^2_{training}	R^2_{testing}
1	0.991	0.006	0.983	0.845
2	0.997	0.0019	0.995	0.964
3	0.998	0.001	0.998	0.897
4	0.998	0.001	0.997	0.886

The coefficients of efficiency (R^2) are found to be .995 for training and .964 for testing as shown in Figures 4.4 and 4.5. Data used in this analysis have been obtained from Patra et al. (2013). All the data used in the training and the testing are from the same source and are of same nature. Probably, this may be one of the causes for better fitting in both testing and training phase as well. The weights and biases of the network are presented in Table 4.4. These weights and biases can be utilized for interpretation of relationship between the inputs and output, sensitivity analysis and framing an ANN model in the form of an equation. The residual analysis was carried out by calculating the residuals from the experimental reduction factor and predicted reduction factor for training data set. Residual (e_r) can be defined as the difference between the experimental and predicted RF_s value and is given by

$$e_r = RF_i - RF_p \tag{4.4}$$

The residuals are plotted with the experiment number as shown in Figure 4.6. It is observed that the residuals are distributed evenly along the horizontal axis of the plot. Therefore, it can be said that the network is well trained and can be used for prediction with reasonable accuracy.

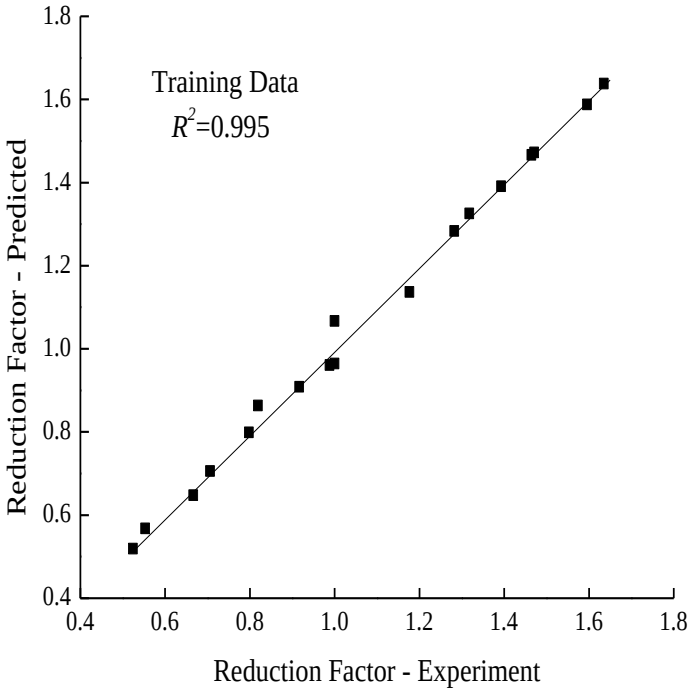

Figure 4.4: Correlation between Predicted Reduction Factor with Experimental Reduction Factor for training data

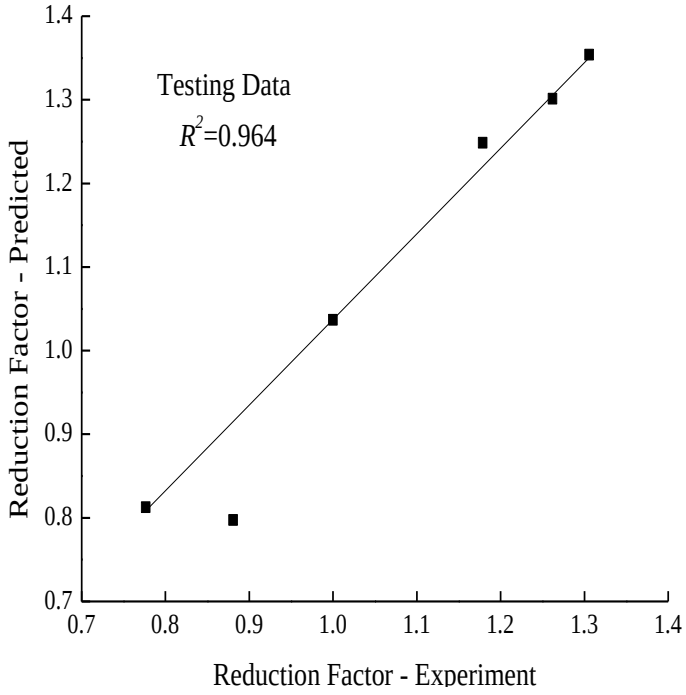

Figure 4.5: Correlation between Predicted Reduction Factor with Experimental Reduction Factor for testing data

Table 4.4: Values of connection weights and biases

Neuron	Weight				Bias	
	w_{ik}			w_k		
	(e/B)	(D_f/B)	D_r	RF_s	b_{hk}	b_0
Hidden Neuron 1 (k=1)	-0.1873	0.1913	0.0254	2.826	-0.3111	1.0679
Hidden Neuron 2 (k=2)	0.9389	1.5548	-0.3068	0.3484	-1.9675	

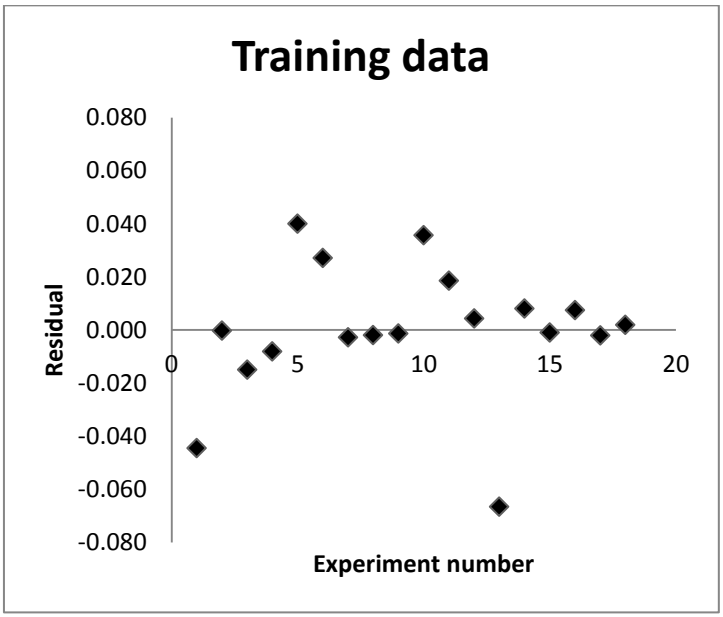

Figure 4.6: Residual distribution of training data

4.5.1 Sensitivity Analysis

Sensitivity analysis is carried out for selection of important input variables. Different approaches have been suggested to select the important input variables. The Pearson correlation coefficient is considered as one of the variable ranking criteria in selecting proper inputs for the ANN. Garson (1991) proposed a method, later on modified by Goh (1995), for partitioning the neural network connection weights in order to determine the relative

importance of each input variable in the network. It is important to mention that Garson's algorithm uses the absolute values of the connection weights when calculating variable contributions, and therefore does not provide the information on the effect of input variables in terms of direct or inverse relation to the output. Olden et al. (2004) proposed a connection weights approach based on the NID, in which the actual values of input-hidden and hidden-output weights are taken. It sums the products across all the hidden neurons, which is defined as S_i. The relative inputs are corresponding to absolute S_i values, where the most important input corresponds to highest S_i value. The details of connection weight approach are presented in Olden et al. (2004).

Table 4.5: Cross-correlation of the input and output for the reduction factor

Parameters	*e/B*	D_f/B	D_r	RF_s
e/B	1	0.044	-.036	-0.452
D_f/B		1	0	0.848
D_r			1	.046
RF				1

Table 4.5 shows the cross correlation of inputs with the reduction factor. From the table it is observed that RF_s is highly correlated to D_f/B with a cross correlation values of 0.848, followed by *e/B* and D_r. The relative importance of the three input parameters as per Garson's algorithm is presented in Table 4.6. The D_f/B is found to be the most important input parameter with the relative importance value being 51.44% followed by 39.94% for *e/B* and 8.62% for D_r. The relative importance of the present input variables, as calculated following the connection weight approach (Olden et al. 2004) is also presented in Table 4.6. The D_f/B is found to be the most important input parameter (S_i value =1.08) followed by D_r

(S_i value = 0.035) and *e/B* (S_i value = -0.2022). The S_i values being positive imply that both D_r and D_f/B are directly and *e/B* is indirectly related to RF_s values.

Table 4.6: Relative Importance of different inputs as per Garson's algorithm and Connection weight approach

Parameters	Garson's algorithm		Connection weight approach	
(1)	Relative Importance (%) (2)	Ranking of inputs as per relative importance (3)	S_i values as per Connection weight approach (4)	Ranking of inputs as per relative importance (5)
e/B	39.94377	2	-0.2022	2
D_f/B	51.43507	1	1.082306	1
D_r	8.621158	3	0.03511	3

4.5.2 Neural Interpretation Diagram (NID)

Ozesmi and Ozesmi (1999) proposed the Neural Interpretation Diagram (NID) for providing a visual interpretation of the connection weights among neurons, where the relative magnitude of each connection weight is represented by line thickness (i.e. magnitude of weights is proportional to line thickness) and line shading represents the direction of the weight (i.e. solid lines denote positive, excitatory signals and dashed lines denote negative, inhibitor signals). The relationship between the inputs and outputs is determined in two steps since there are input-hidden layer connections and hidden-output layer connections. Positive effects of input variables are depicted by positive input-hidden and positive hidden-output connection weights, or negative input-hidden and negative hidden-output connection weights. Negative effects of input variables are depicted by positive input-hidden and negative hidden-output connection weights, or by negative input-hidden and positive hidden-output connection weights. Therefore, the multiplication of the two connection weight directions (positive or negative) indicates the effect that each input variable has on the output variable.

The input directly related to the output is represented with a grey circle and that having inverse effect with blank circle.

It is seen from Table 4.6. (4th Column) that S_i values for parameter (e/B) being negative indicating that (e/B) is inversely related to RF_s values, whereas S_i value for parameters D_r and D_f/B are positive indicating that both the parameters are directly related to RF_s values. This is shown in Figure. Therefore, the developed ANN model is not a "black box" and could explain the physical effect of the input parameters on the output.

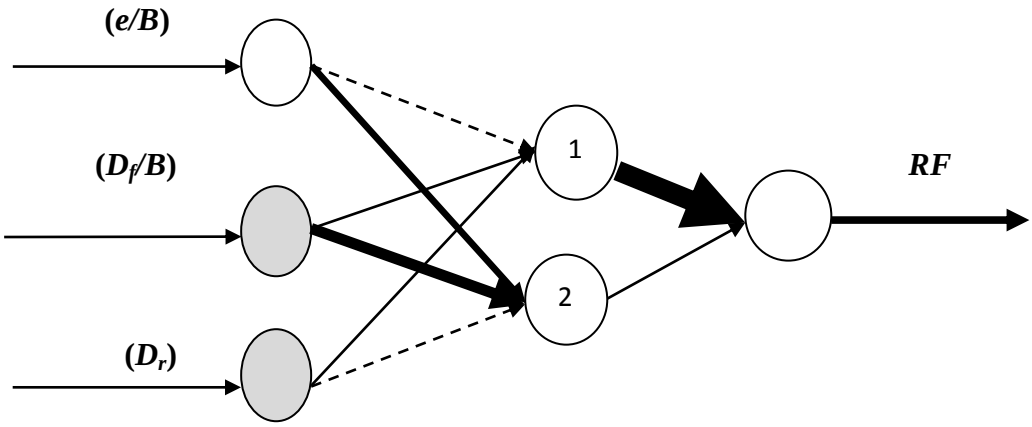

Figure 4.7: Neural Interpretation Diagram (NID) showing lines representing connection weights and effects of inputs on Reduction Factor (RF_s)

4.5.3 ANN model equation for the Reduction Factor based on trained neural network

A model equation is developed with the weights obtained from trained neural network as the model parameters (Goh et al. 2005). The mathematical equation relating input parameters (e/B, D_f/B, and D_r) to output (Reduction Factor) can be given by

$$RF_{s(n)} = f_n \left\{ b_0 + \sum_{k=1}^{h} \left[w_k \, f_n \left(b_{hk} + \sum_{i=1}^{m} w_{ik} X_i \right) \right] \right\} \tag{4.5}$$

where $RF_{s(n)}$= normalized value of RF_s in the range [-1, 1], f_n = transfer function, h = no. of neurons in the hidden layer, X_i= normalized value of inputs in the range [-1, 1], m = no. of input variables, w_{ik} = connection weight between i^{th} layer of input and k^{th} neuron of hidden layer, w_k = connection weight between k^{th} neuron of hidden layer and single output neuron, b_{hk} = bias at the k^{th} neuron of hidden layer, and b_o = bias at the output layer.

The model equation for Reduction Factor of shallow strip foundations subjected to eccentric load was formulated using the values of the weights and biases shown in as per the following steps.

Step – 1

The input parameters were normalized in the range [-1, 1] by the following expressions

$$X_n = 2\left(\frac{X_1 - X_{\min}}{X_{\max} - X_{\min}}\right) - 1 \tag{4.6}$$

where, X_n= Normalized value of input parameter X_1, and X_{max} and X_{min} are maximum and minimum values of the input parameter X_1 in the data set.

Step – 2

Calculate the normalized value of reduction factor ($RF_{s\,(n)}$) using the following expressions

$$A_1 = -0.1873\left(\frac{e}{B}\right)_n + 0.1913\left(\frac{D_f}{B}\right)_n + 0.0254(D_r)_n - 0.3111 \tag{4.7}$$

$$A_2 = 0.9389\left(\frac{e}{B}\right)_n + 1.5548\left(\frac{D_f}{B}\right)_n - 0.3068\left(\frac{\alpha}{\phi}\right)_n - 1.9675 \tag{4.8}$$

$$B_1 = 2.8260\left(\frac{e^{A_1} - e^{-A_1}}{e^{A_1} + e^{-A_1}}\right) \tag{4.9}$$

$$B_2 = .3484\left(\frac{e^{A_2} - e^{-A_2}}{e^{A_2} + e^{-A_2}}\right) \tag{4.10}$$

$$C_1 = 1.0679 + B_1 + B_2 \tag{4.11}$$

$$RF_n = C_1 \tag{4.12}$$

$$RF_{s(n)} = f_{sig}\left\{b_0 + \sum_{k=1}^{h}\left[w_k\, f_{sig}\left(b_{hk} + \sum_{i=1}^{m} w_{ik} X_i\right)\right]\right\} \tag{4.13}$$

Step – 3

Denormalize the RF_n value obtained from Eq. (4.12) to actual RF as

$$RF = 0.5(RF_n + 1)(RF_{\max} - RF_{\min}) + RF_{\min} \tag{4.14}$$

$$RF = 0.5*(RF_n + 1)*(1.635 - 0.524) + 0.524 \tag{4.15}$$

4.6. Comparison with Patra et al. (2013)

Patra et al. (2013) proposed a reduction factor (RF) for estimation of ultimate settlement of eccentrically loaded strip footing which is given by

$$RF \approx \left[1 + 0.6\left(\frac{D_f}{B}\right)\right]\left[1 - 2.15\left(\frac{e}{B}\right)\right] \tag{4.16}$$

For comparison, the RF values calculated based on Eq. (4.16) are presented in Table 1 (9^{th} column) and plotted along with Eqs. (4.15) and (4.1) in Figure 4.8. It can be observed clearly from the Figure that RF values based on present analysis is much closer to line of equality than the empirical one proposed by Patra et al. (2013).

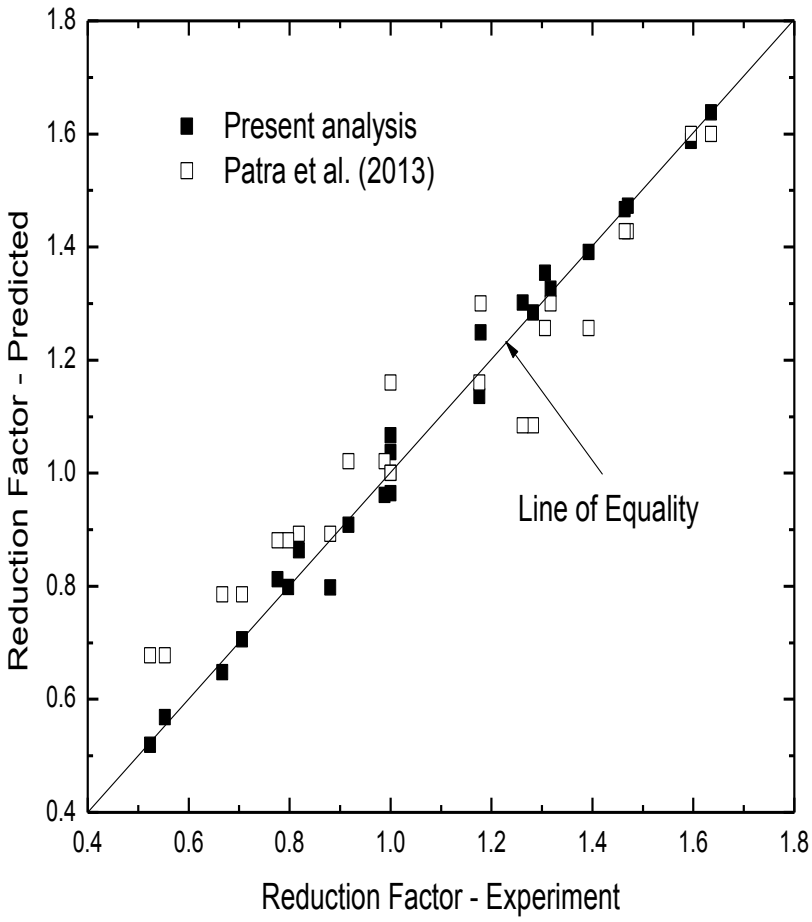

Figure 4.8: Comparison of RF_s values obtained from present analysis with Patra et al. (2013)

4.7. Conclusions

Based on developed neural network model, the following conclusions are drawn:

- As per residual analysis, the errors are distributed evenly along the horizontal axis. It can be concluded that the network is well trained and can predict the result with reasonable accuracy.
- Based on Pearson correlation coefficient and Garson's algorithm, it was observed that D_f/B is the most important input parameter followed by e/B and D_r.
- As per connection weight approach, D_f/B is found to be the most important input parameter followed by D_r and e/B. Based on the analysis, Hence, it may be concluded that sensitivity analysis using Connection weight approach is able to explore the inputs-output relationship using trained weights.

- The developed ANN model could explain the physical effect of inputs on the output, as depicted in NID. It was observed that e/B was inversely related to RF_s values whereas D_f/B and D_r were directly related to RF_s.
- A model equation is developed based on trained weights of the Ann.
- The predictability of settlement by ANN model is better than the empirical equation proposed by Patra et al. (2013).

CHAPTER V

RESULTS AND DISCUSSION

5.1 Introduction

Model tests have been conducted in the laboratory using square footings with embedment ratio D_f /B varying from zero to one, the eccentricity ratio e/B varying from zero to 0.15 [Figure 5.1]. In order to investigate the effect of load eccentricity on the load carrying capacity of square embedded footings, laboratory model tests have been conducted on footings supported by dry sand bed. The test results have been used to develop nondimensional reduction factor which may be used for estimating the ultimate bearing capacity of eccentrically loaded footings from bearing capacity of centrally loaded footings. The developed empirical equation is compared with Meyerhof's theory.

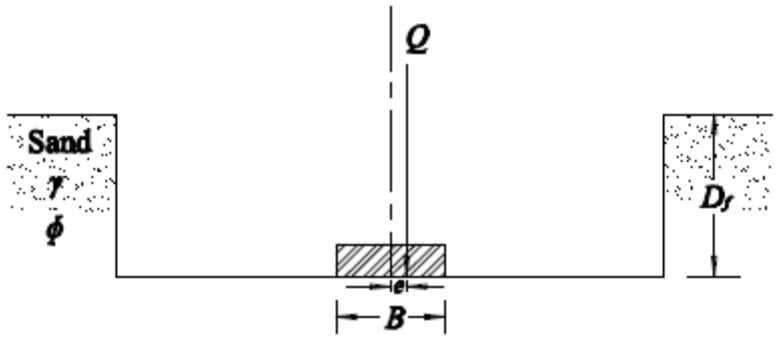

Figure 5.1: Eccentrically loaded Square footing

Based on a review of published theoretical and experimental studies related to the estimation of ultimate bearing capacity of square foundation subjected to eccentric load, it shows that very less efforts have been paid for finding out effect of eccentricity on square or rectangular footings. Experimental results in this direction are scanty. Hence it is evident that further efforts are needed to quantify certain parameters.

Purkayastha and Char (1977) proposed the reduction factor corresponding to ultimate bearing capacity for eccentrically loaded strip footing as follows:

$$R_k = 1 - \frac{q_{u(eccentric)}}{q_{u(centric)}} \qquad (5.1)$$

where R_k = reduction factor; $q_{u(eccentric)}$ = ultimate bearing capacity of eccentrically loaded continuous foundations; $q_{u(centric)}$ = ultimate bearing capacity of centrally loaded continuous foundations.

Therefore, based on the concept in Eq. (5.1) for load eccentricity it shows that a reduction factor *RF* for square footing can be developed for a given value of D_f/B.

$$RF = \frac{q_{u\left(e/B\,,D_f/B\right)}}{q_{u\left(e/B=0,D_f/B\right)}} \qquad (5.2)$$

where $q_{u(e/B\,,D_f/B)}$ =ultimate bearing capacity with eccentricity ratio e/B at an embedment ratio D_f/B and $q_{u(e/B=0,D_f/B)}$= ultimate bearing capacity with centric vertical loading (e/B = 0) at the same embedment ratio D_f/B.

Thus it can initially be assumed that

$$RF = 1 - b\left(\frac{e}{B}\right)^n \qquad (5.3)$$

where b, n = factors which are functions of D_f/B.

The purpose of this chapter is to conduct laboratory model tests on square foundations with varying D_f/B and e/B with 69% relative density and evaluate the coefficients b and n as given in Eq. (5.3).

5.2. Centric Loading Conditions

The model tests are performed (i.e. e/B = 0) in centric vertical loading condition. The details of the test parameters are shown in Table 5.1. Basically there are five different methods to interpret the ultimate bearing capacity from the load-settlement curve namely Log-Log

method (DeBeer 1970), Tangent Intersection method (Trautmann and Kulhawy 1988), 0.1*B* method (Briaud and Jeanjean 1994), Hyperbolic method (Cerato 2005), and Break Point method (Mosallanezhad et al. 2008). For the present test results, the ultimate bearing capacity is determined by Tangent Intersection method [Figure 5.2].

Table 5.1: Model test parameters for the case of Centric Loading condition

B/L	Sand type	Unit weight (kN/m³)	Relative Density of sand %	Friction angle φ- direct shear test (degree)	D_f/B	e/B
1	Dense	14.36	69	40.8	0 0.5 1.0	0
0.5	Dense	14.36	69	40.8	0	0

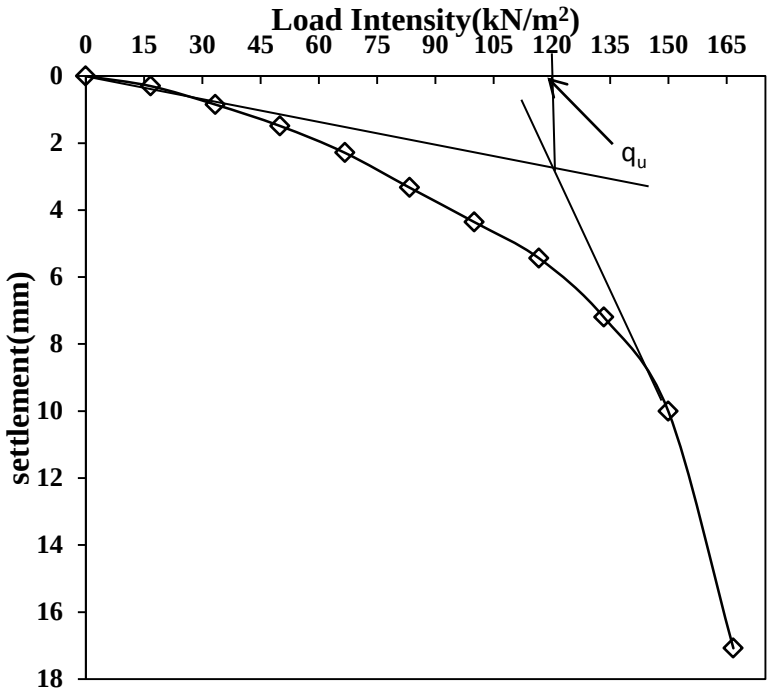

Figure 5.2: Interpretation of Ultimate bearing capacity q_u by Tangent Intersection method

5.2.1 Surface Footing with Centric Loading Conditions

For 10cmx10cm size footing it is observed that for central loading definite failure point is observed. This curve shows the characteristics of General shear failure. Tangent intersection method is used to obtain ultimate bearing capacity of footing. It is found that for centrally loaded Square footing ultimate bearing capacity, q_u is 121 kN/m^2. For 10cm x 20cm sizes rectangular footing it is observed that for central loading a definite failure point is observed as shown in Fig. 5.4. This curve also shows the characteristics of General shear failure. It is found that for centrally loaded rectangular footing ultimate bearing capacity; q_u is 125 kN/m^2.

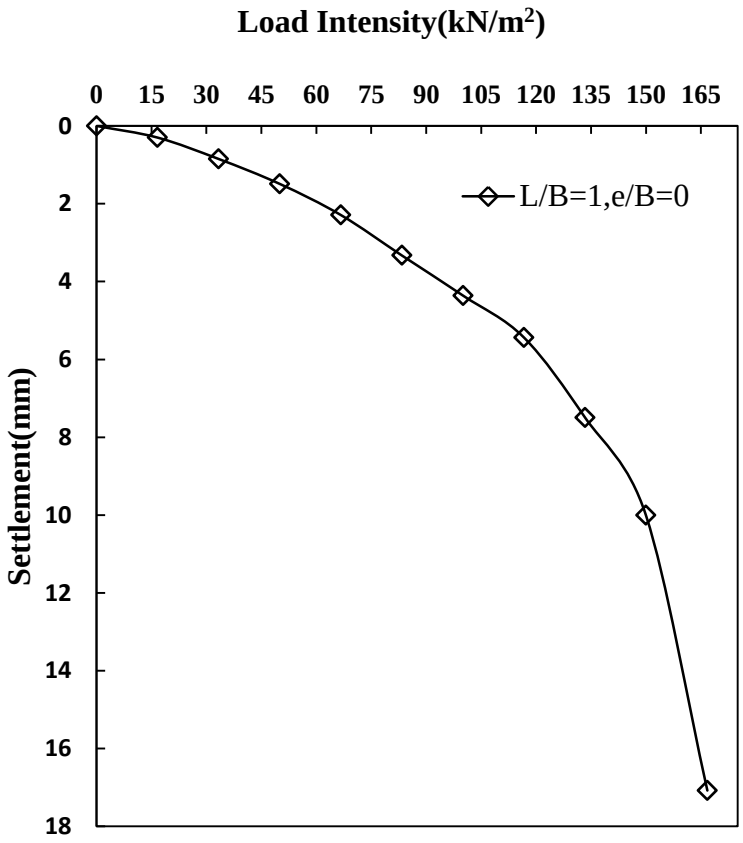

Figure 5.3: Load Intensity vs. Settlement curve for Footing size 10cmx10cm at D_f/B=0

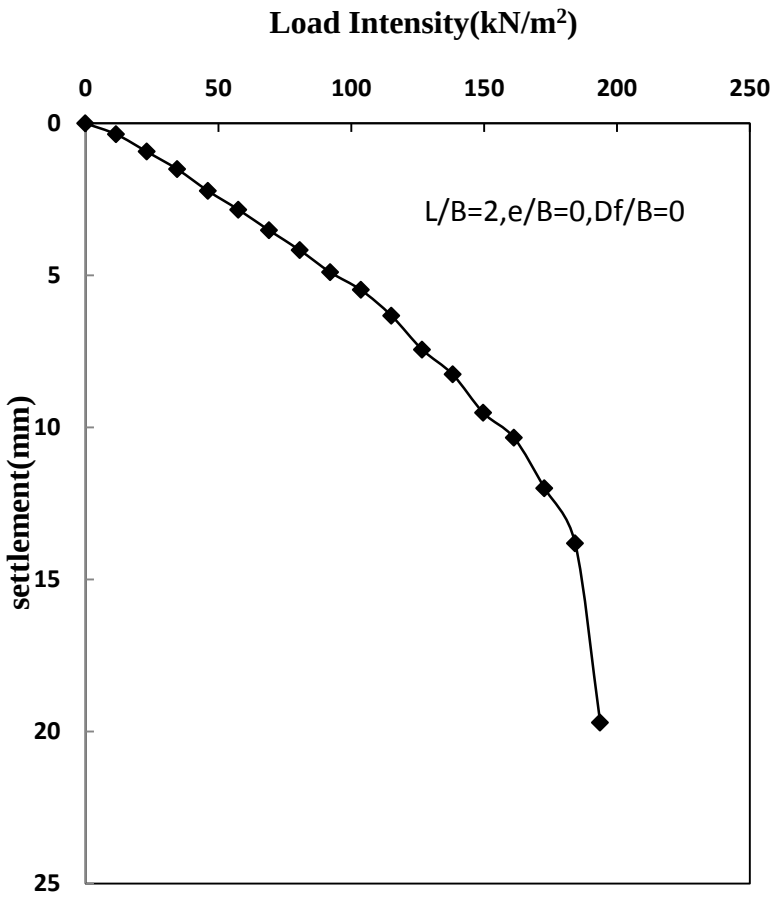

Figure 5.4: Load Intensity vs. Settlement curve for Footing size 10cmx20cm

5.2.2 Embedded Footing at Centric Loading Conditions

The load settlement curve corresponding to (D_f /B=0, 0.5, 1.0) are obtained from the experimental results. The combined load settlement curves to D_f /B=0, 0.5, 1.0 curve are shown in figure 5.5. As seen in Figures 5.5, the bearing capacity of square footing increases with the increase in depth of embedment. The ultimate bearing capacity for 0.5B depth of embedment is 238 kN/m^2 at centric loading condition (e/B=0). Similarly for 1B depth of embedment at centric loading condition the ultimate bearing capacity is 339 kN/m^2.

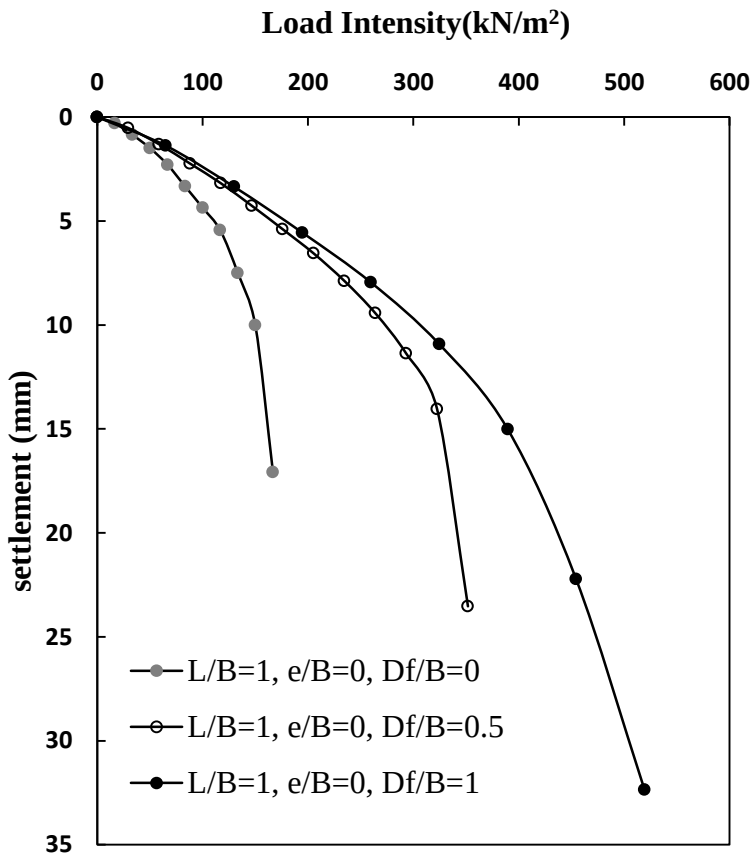

Figure 5.5: Variation of load-settlement curve with embedment ratio (D_f/B) at e/B=0

The theoretical values of ultimate bearing capacities corresponding to ϕ=40.8° for the case of centric loading (e/B = 0) at various depth of embedment i.e. D_f/B = 0, 0.5 and 1.0 have been obtained using the expressions mentioned in section 2.2 for Meyerhof (1951), Terzaghi (1943), Hansen (1970), Vesic (1973). These values are plotted in Figure 5.6. The same has been presented in Table 5.2 and 5.3. In figure 5.6 along with the theoretical values; the present experimental values are shown.

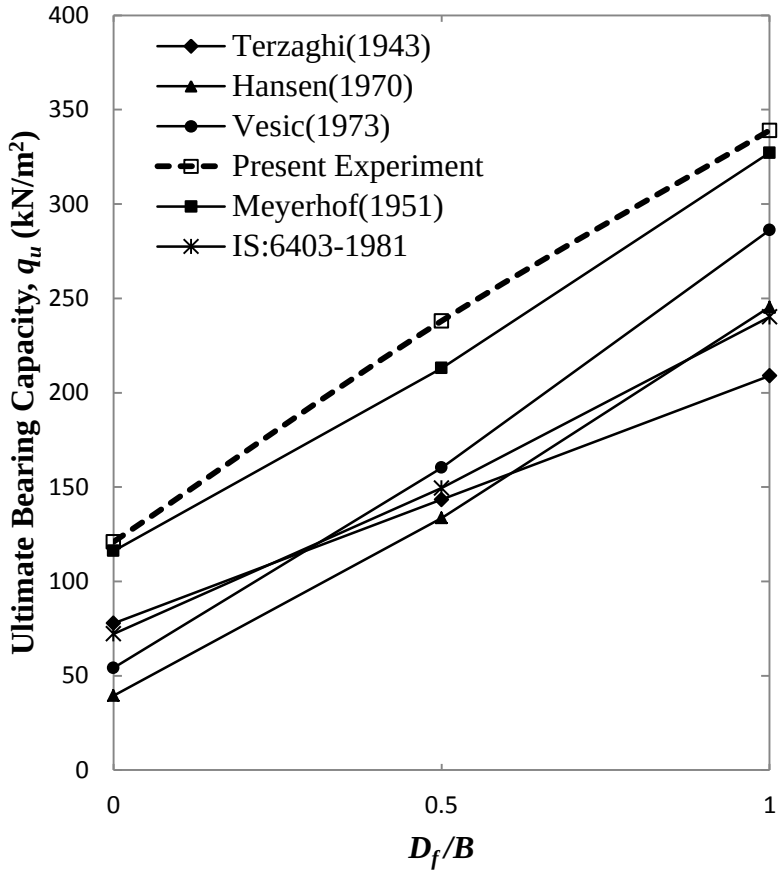

Figure 5.6: Variation of q_u with D_f/B for $e/B = 0$ using formulae of existing theories along with present experimental values

It is seen from the Fig. 5.6 that that experimental bearing capacities for a given D_f /B are significantly higher than those predicted by theories except Meyerhof's method. Bearing-capacity model tests of shallow footings carried out in various geotechnical laboratories clearly showed that model test results are, in general, much higher than those calculated by traditional methods (Balla 1962; Bolt 1982; Cichy et al. 1978; Ingra and Baecher 1983; Hartikainen and Zadroga 1994; Milovic 1965; Saran and Agarwal 1991; Shiraishi 1990; Zadroga 1975). There are several reasons for this, the most important of which is the unpredictability of N_γ and the scale effect associated with the model tests. DeBeer (1965) compiled several bearing capacity test results which are shown in Figure 5.7 as a plot of N_γ vs. γB. The value of N_γ rapidly decreases with the increase in γB. DeBeer (1965) also

compared the variation of N_γ obtained from small scale laboratory and large scale field test results, and these are given in Fig. 5.8.

Table 5.2: Calculated values of ultimate bearing capacities q_u by Terzaghi (1943) and Meyerhof (1951) for centric vertical condition along with Present experimental values

e/B	D_f/B	Present Experiment; q_u (kN/m^2)	Meyerhof (1951); q_u (kN/m^2)	Terzaghi (1943); q_u (kN/m^2)
		ϕ =40.8°	ϕ =40.8°	ϕ =40.8°
0	0	121	116.2	77.81
	0.5	238	213	143.4
	1	339	327.1	209

Table 5.3: Calculated values of ultimate bearing capacities q_u by Hansen (1970) and Vesic (1973) for centric vertical condition along with Present experimental values

e/B	***D_f/B***	Present Experiment; q_u (kN/m^2)	Hansen (1970); q_u (kN/m^2)	Vesic (1973); q_u (kN/m^2)
		ϕ =40.8°	ϕ =40.8°	ϕ =40.8°
0	0	121	39.5	54.164
	0.5	238	133.625	160.25
	1	339	245.31	245.31

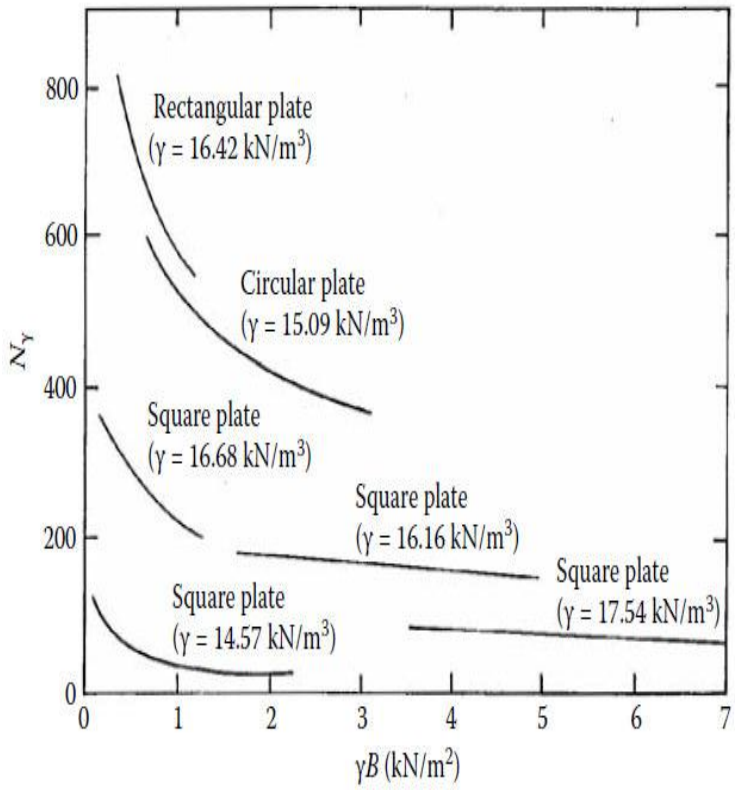

Figure 5.7: Variation of N_γ with γB (adapted after DeBeer, 1965)

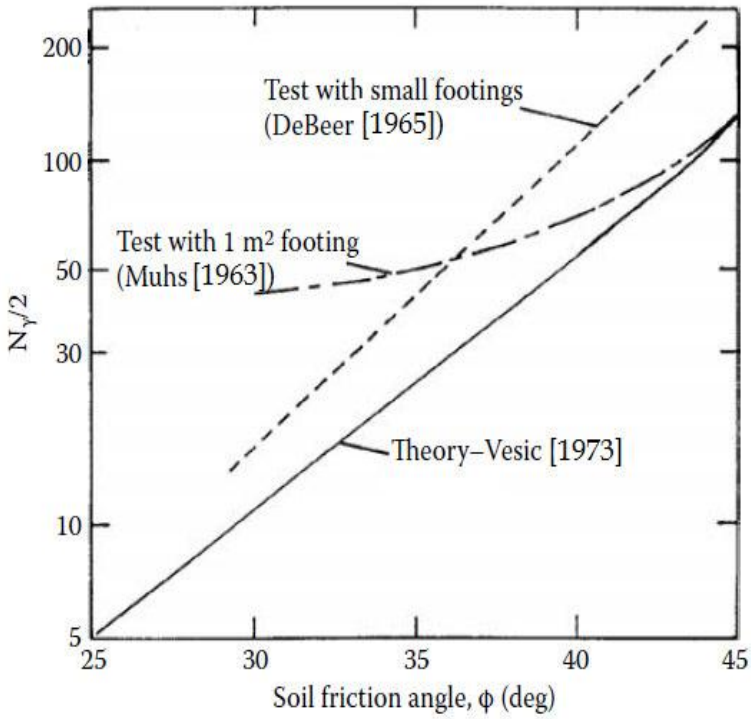

Figure 5.8: Comparison of N_γ obtained from tests with small footings and large footings of 1m² area on sand (adapted after DeBeer, 1965).

Figure 5.9: Photographic image of failure pattern of centric loaded square footing at 1.0*B* depth of embedded

5.3 Eccentric Loading Conditions

Twelve numbers of model tests are conducted in eccentric loading condition. The load settlement curves of square foundations (*e/B* = 0, 0.05, 0.1 and 0.15) in surface condition are plotted in Figure 5.10. The load carrying capacity decreases with increase in *e/B* ratio. Similarly, Fig.5.14 through 5.17 shows the variation of load-settlement curve with depth of embedment (D_f/B).

5.3.1 Surface Footing at Eccentric Loading Conditions

The ultimate bearing capacity of square footings (10cm x 10cm) with eccentric loading of (*e/B* = 0.05, 0.1, and 0.15) has been found out. The values obtained are presented in Table 5.5 (col.2) and shows in Fig.5.10. Similarly, for surface rectangular footing with load eccentricities the ultimate bearing capacities have been computed and shown in Figure 5.12. It is found that for eccentric loading of 10cm x 20 cm size rectangular footing i.e. e/B=0.05, 0.1, 0.15 the ultimate bearing capacities are 114 kN/m^2, 100 kN/m^2 and 90 kN/m^2

respectively. It is observed that the Ultimate Bearing Capacity decreases with increase in eccentricity both in square as well as rectangular footing.

Table 5.4: Model test parameters for the case of Eccentric Loading condition

B/L	Sand type	Unit weight (kN/m³)	Relative Density of sand %	Friction angle φ- direct shear test (degree)	D_f/B	e/B
1	Dense	14.36	69	40.8	0 0.5 1.0	0 0.05 0.1 0.15
0.5	Dense	14.36	69	40.8	0	0 0.05 0.1 0.15

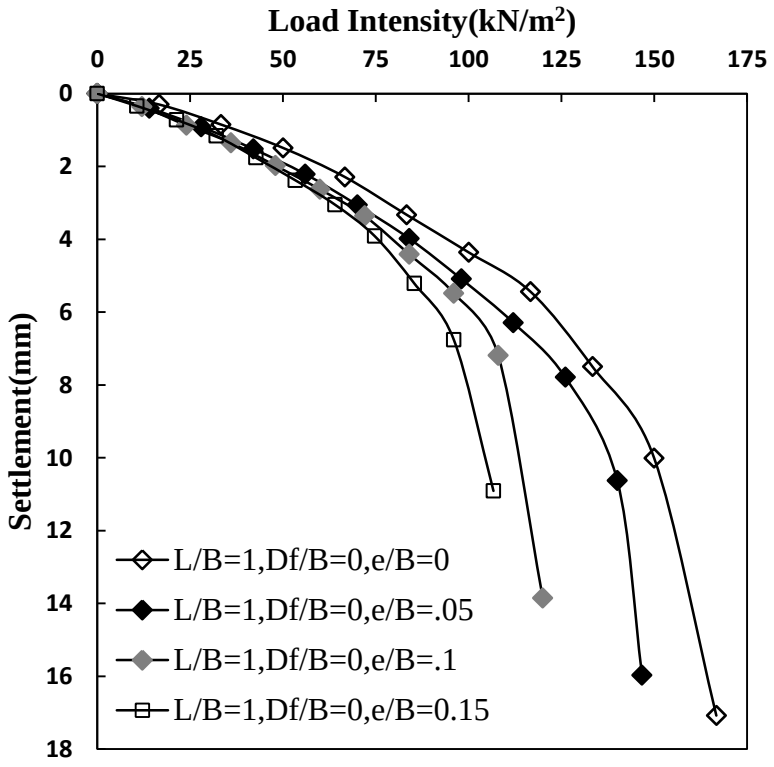

Figure 5.10: Load Intensity vs. Settlement Curve for Footing size 10cmx10cm with e=0, 0.05B, 0.1B and 0.15B

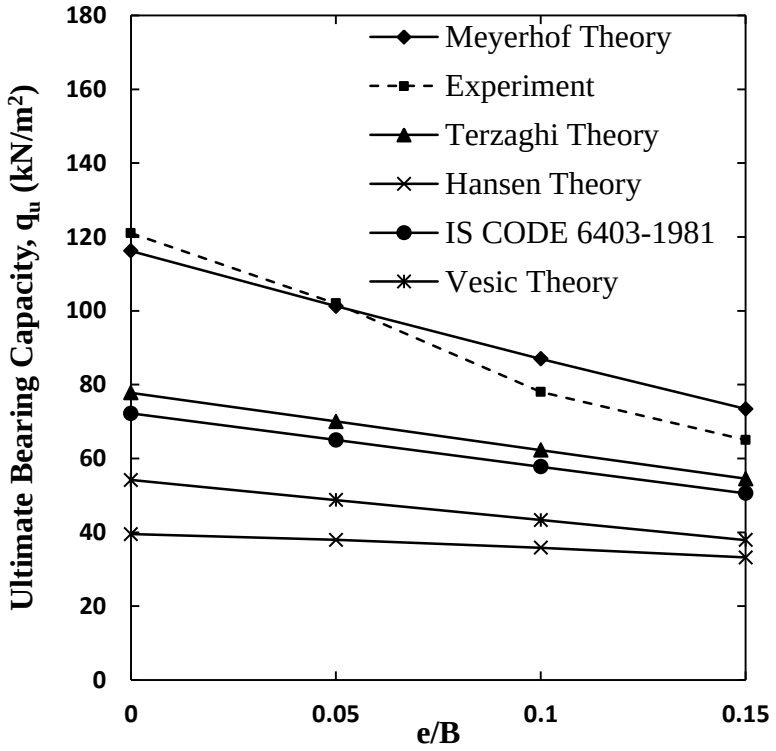

Figure 5.11: Comparison of ultimate bearing capacities of Present experimental results with different available theories

Table 5.5: Calculated values of ultimate bearing capacities (q_u) by different theories for eccentric condition along with Present experimental values at surface condition

e/B	present Experiment; q_u (kN/m^2)	Terzaghi (1943); q_u (kN/m^2)	Meyerhof (1953); q_u (kN/m^2)	Hansen (1970); q_u (kN/m^2)	Vesic (1973); q_u (kN/m^2)	Is code 6430-1981; q_u (kN/m^2)
(1)	(2)	(3)	(4)	(5)	(6)	(7)
0	121	77.81	116.2	39.5	54.164	72.219
0.05	102	70.03	101.24	37.927	48.748	64.997
0.1	78	62.25	86.97	35.820	43.3315	57.775
0.15	67	54.5	73.423	33.186	37.915	50.553

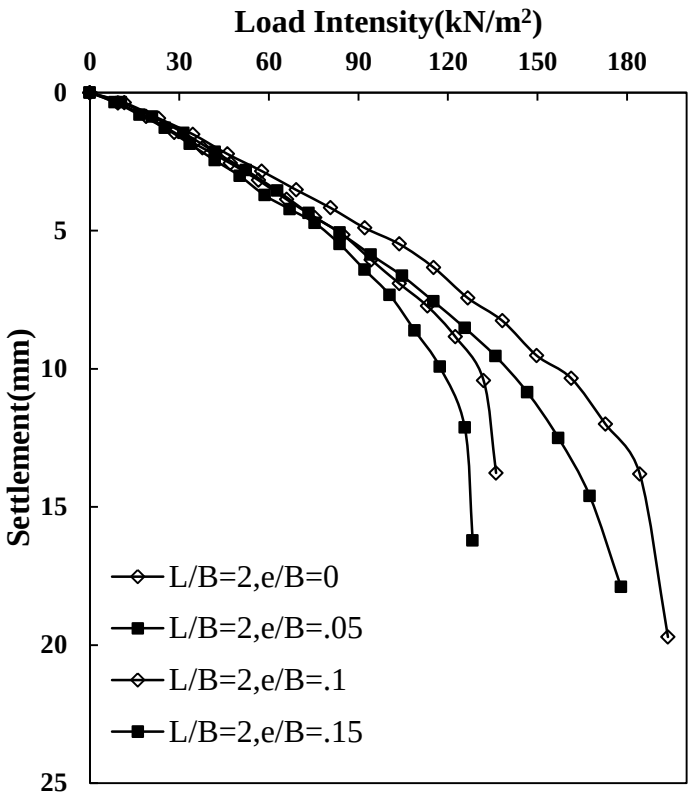

Figure 5.12: Load Intensity vs. Settlement for Footing size 10cmx20cm with *e*=0, 0.05*B*, 0.1*B* and 0.15*B*

5.3.2 Embedded Footing at Eccentric Loading Conditions

Load-settlement curves have been plotted for the case of eccentrically embedded footing to show the effect of embedment and effect of eccentricity. These are shown in Figs. 5.13 through 5.17. It is seen from the Figs. 5.13 and 5.14 that at depth of embedment equal to 0.5B or 1.0B, the bearing pressure at any settlement level decreases with increase in eccentricity like surface footing. Similarly, Figs. 5.15 through 5.17 indicate that at any eccentricity, the bearing pressure increases with increase in depth of embedment at any level of settlement. The ultimate bearing capacities of eccentrically loaded square footings (10cm x 10cm) at 0.5B and 1B depth of embedment have been found out. The values obtained are presented in Table 5.6 (col.3). The same has been shown in Figs.5.13 and 5.14. It is seen that the ultimate bearing capacity of footing increases with the increase in depth of embedment at any

eccentricity. Similarly, at any depth of embedment, the ultimate bearing capacity decreases with increase in eccentricity.

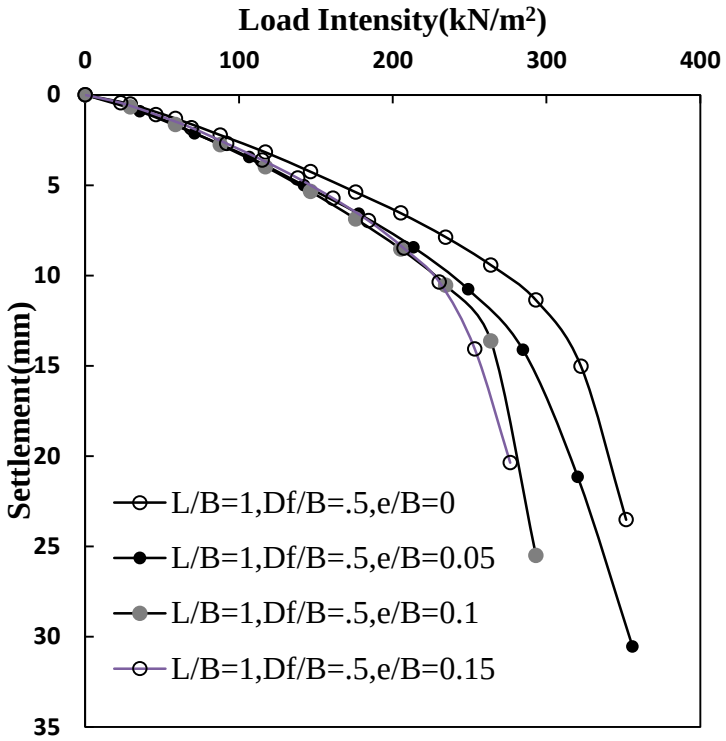

Figure 5.13: Variation of load-settlement curve with eccentricity and D_f = 0.5B condition

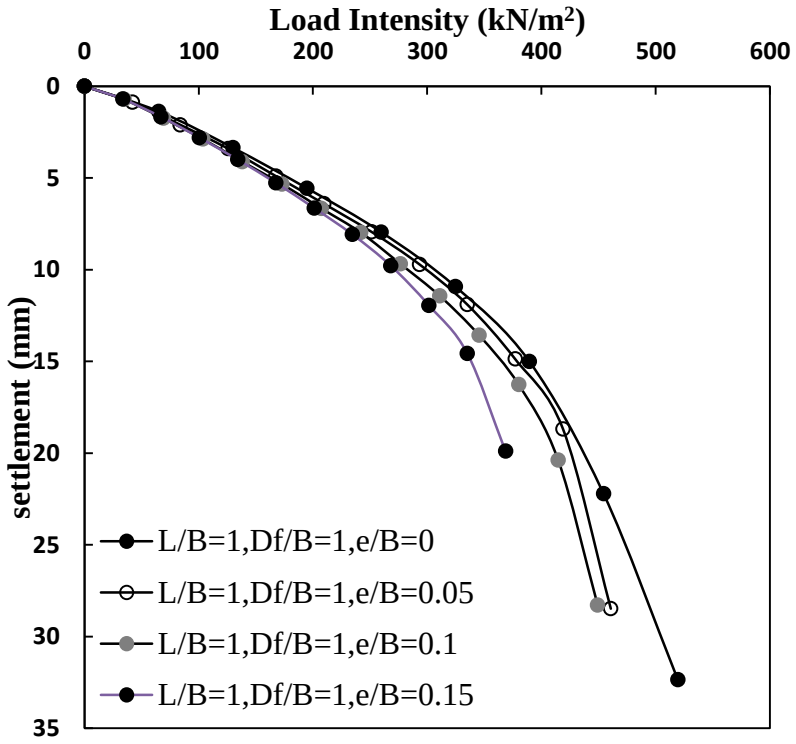

Figure 5.14: Variation of load-settlement curve with eccentricity and (D_f = 1B) Condition

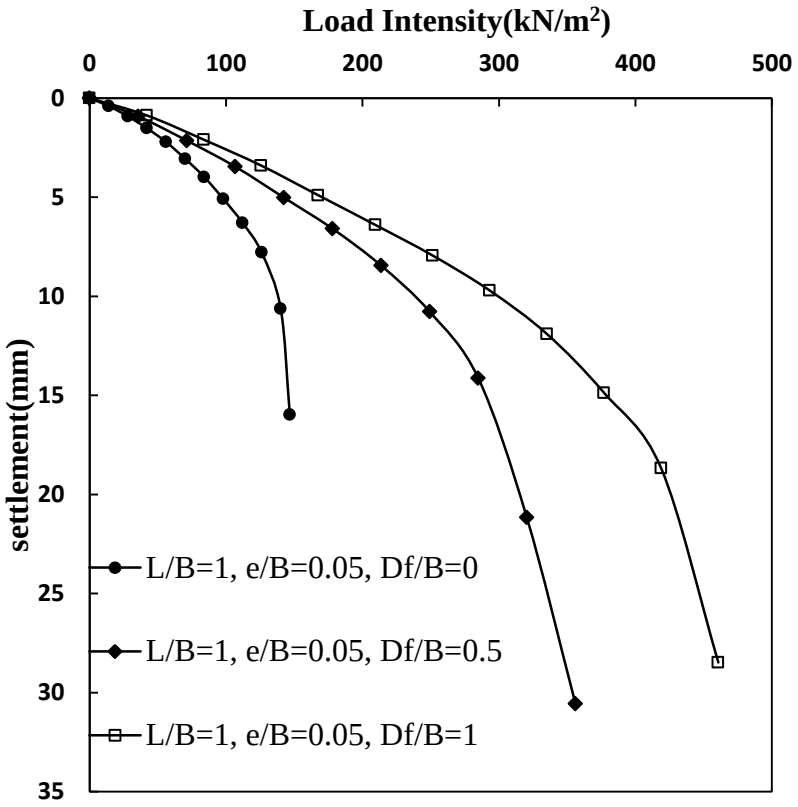

Figure 5.15: Variation of load-settlement curve with embedment ratio (D_f/B) at e/B=0.05

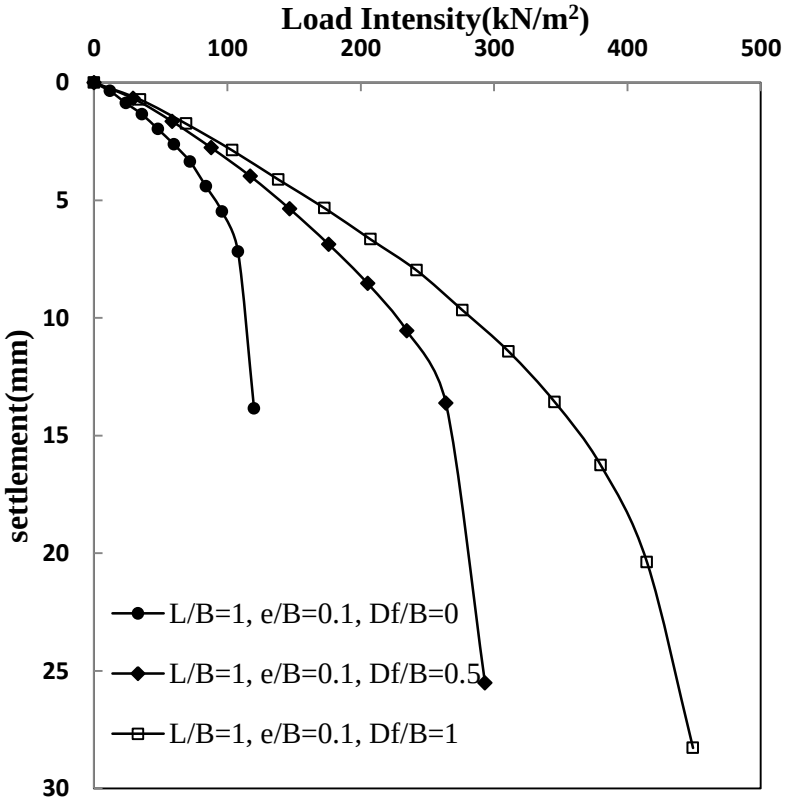

Figure 5.16: Variation of load-settlement curve with embedment ratio (D_f/B) at e/B=0.1

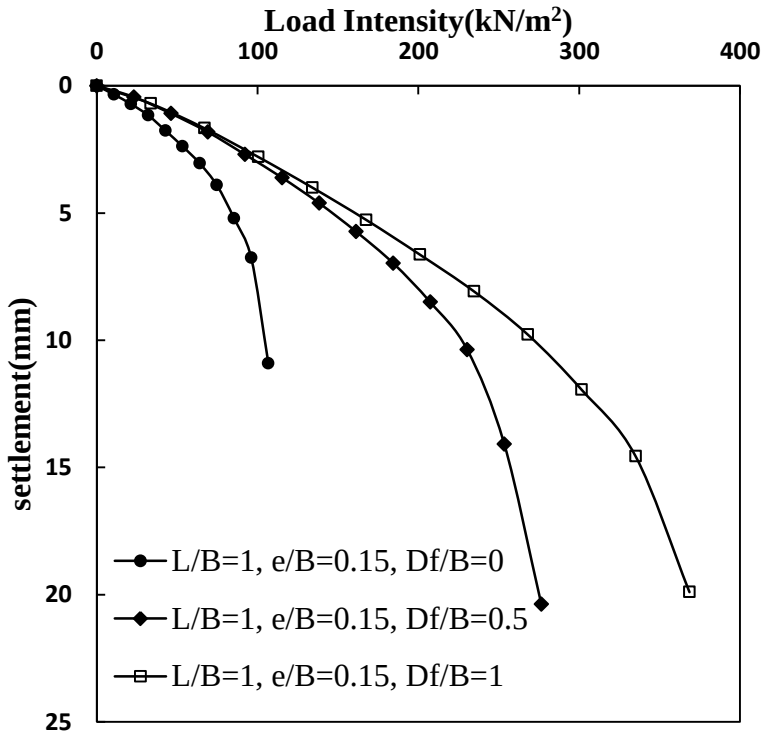

Figure 5.17: Variation of load-settlement curve with embedment ratio (D_f/B) at e/B=0.15

The experimental ultimate bearing capacities for eccentrically loaded foundations (e/B = 0, 0.05, 0.1 and 0.15, D_f/B = 0, 0.5 and 1) are plotted along with the bearing capacities obtained by using Meyerhof's effective area method (Eq. 2.6). This is shown in Figure 5.18 and Table 5.5. The nature of decrease of bearing capacity with the increase in eccentricity as observed from experimental results are with those using Meyerhof's method (1953). It can be seen from Fig. 5.18 that the difference in experimental UBC and computed UBC by Meyerhof's method is more at higher eccentricity and higher depth of embedment. Michalowski and You (1998) revealed that for purely frictional (granular) soil and relatively small surcharge loads, the effective width rule over- estimates the best upper bound to the average bearing pressure. Also for a surface footing with eccentricity e/B =0.25 this overestimation is 35%, and it increases with an increase in e/B. Yamamoto and Hira (2009) also used finite elements to calculate the bearing capacity of surface foundations on frictional soils under eccentric loadings, and for a friction angle of 35° and an eccentricity e = (1/3) B, they found a bearing capacity equal to about 45% of the one determined by the effective width approach.

Table 5.6: Calculated values of (q_u) by Meyerhof (1953) for eccentric condition along with Present experimental values of q_u

D_f/B (1)	e/B (2)	Present Experiment; q_u (kN/m^2) (3)	Meyerhof (1953); q_u (kN/m^2) (4)
0	0	121	116.2
	0.05	102	101.24
	0.1	78	86.97
	0.15	65	73.42
0.5	0	238	213
	0.05	198	196.22
	0.1	176	179
	0.15	143	164.377
1	0	339	327.5
	0.05	294	309.11
	0.1	258	292.18
	0.15	227	276.78

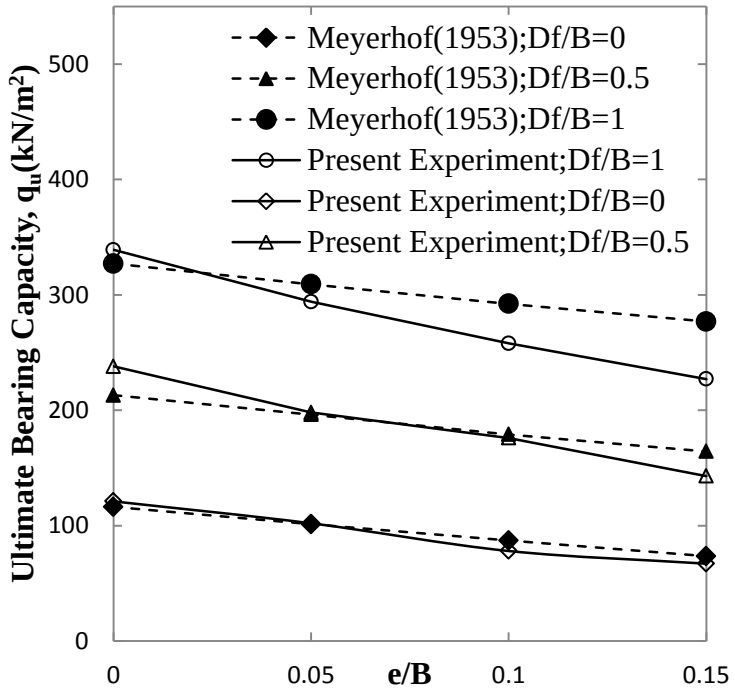

Figure 5.18: Comparison of ultimate bearing capacities of Present experimental results with q_u of Meyerhof (1953)

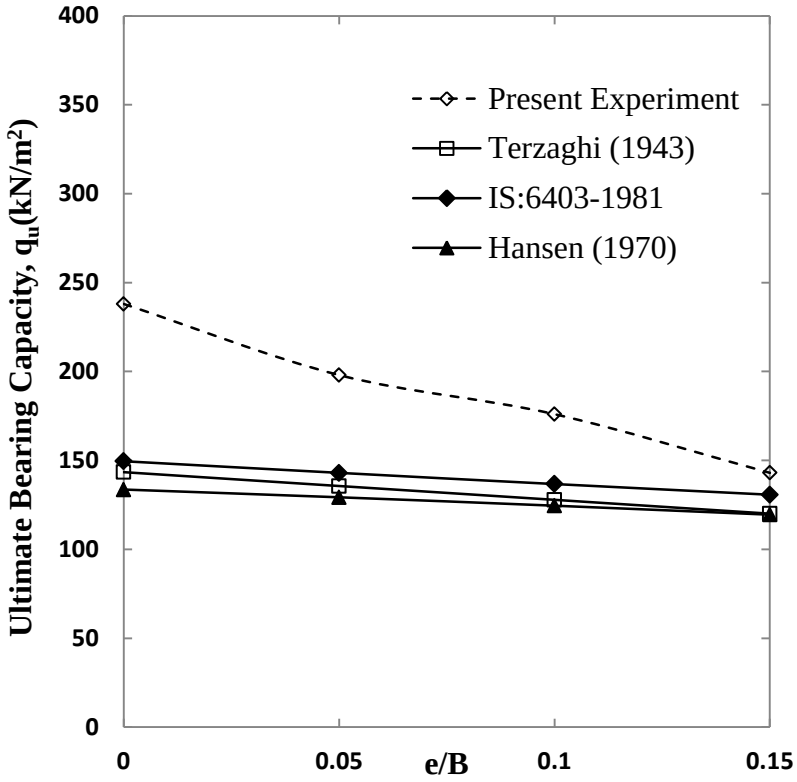

Figure 5.19: Comparison of ultimate bearing capacities of Present experimental results with q_u of different theories at D_f=0.5B

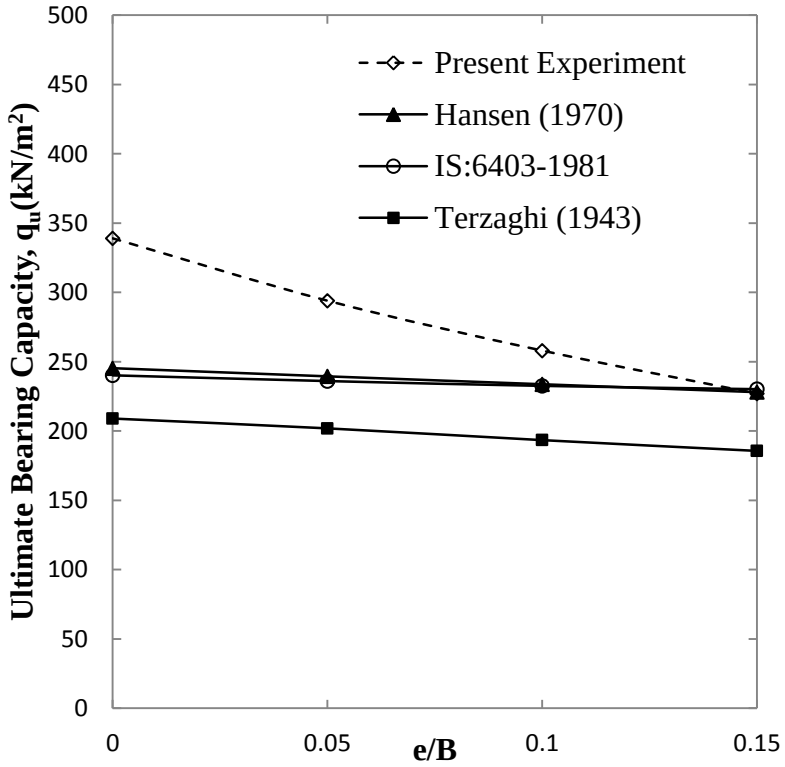

Figure 5.20: Comparison of ultimate bearing capacities of Present experimental results with q_u of different theories at D_f =1.0B

The experimental ultimate bearing capacities for eccentrically loaded foundations are plotted along with the bearing capacities obtained by using different theories at 0.5*B* and 1.0*B* depth of embedment. The values obtained are presented in Table 5.7. The same has been shown in Figs.5.19 and 5.20.

Table 5.7: Calculated values of q_u by different theories for eccentric condition along with Present experimental values

D_f/B (1)	e/B (2)	present Experiment; q_u (kN/m^2) (3)	Terzaghi (1943); q_u (kN/m^2) (4)	Hansen (1970); q_u (kN/m^2) (5)	IS Code 6403-1981; q_u (kN/m^2) (6)
0.5	0	238	143.39	133.625	149.5376
	0.05	198	135.61	129.26	142.9954
	0.1	176	127.83	124.53	136.716
	0.15	143	120.05	119.475	130.701
1	0	339	208.97	245.31	240.16
	0.05	294	201.88	239.43	236.0264
	0.1	258	193.41	233.72	232.553
	0.15	227	185.63	228.012	230.158

The reduction factor (*RF*) obtained from the present experimental data for the square footing has been compared with the *RF* for strip footing as given by Purkayastha and Char at depth of embedment (D_f/B=0, 0.5, 1.0). The reduction factors at all eccentricities and at all depth of embedment are in well close agreement. These are shown in figures 5.21, 5.22 and 5.23.

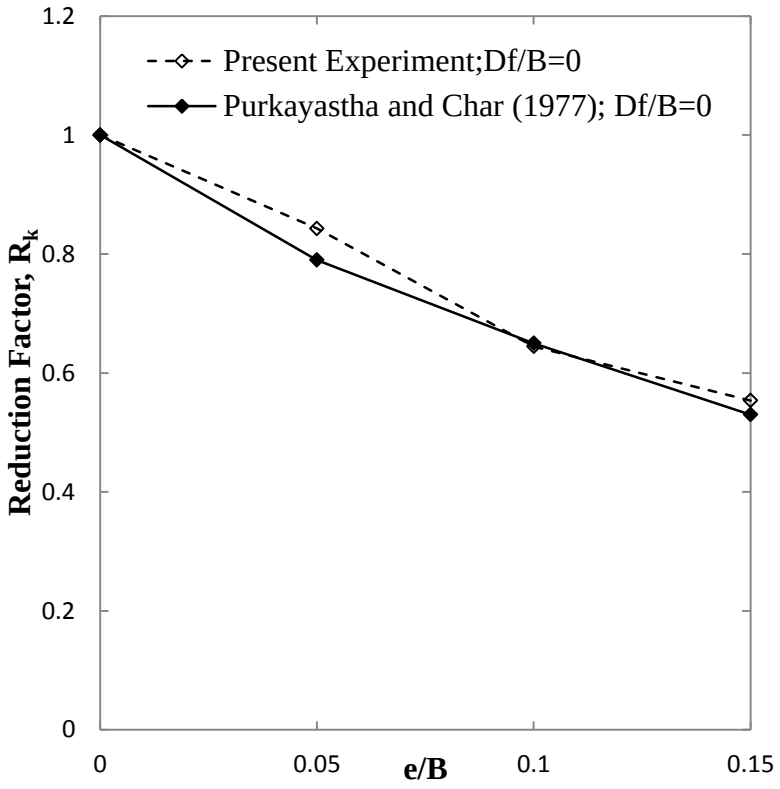

Figure 5.21: Comparison of Present experimental results with Purkayastha and Char (1977) with D_f/B=0

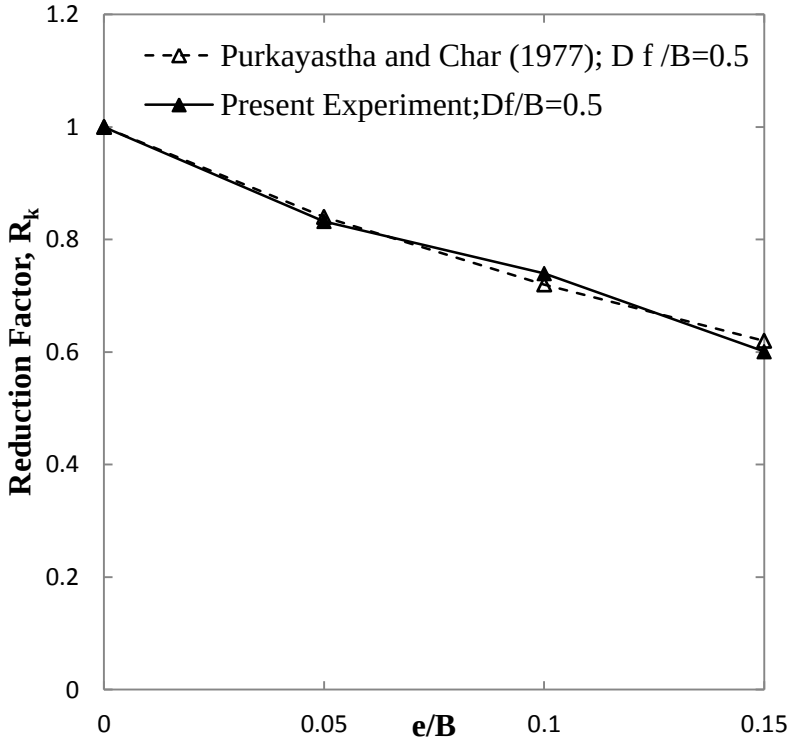

Figure 5.22: Comparison of Present experimental results with Purkayastha and Char (1977) with D_f/B=0.5

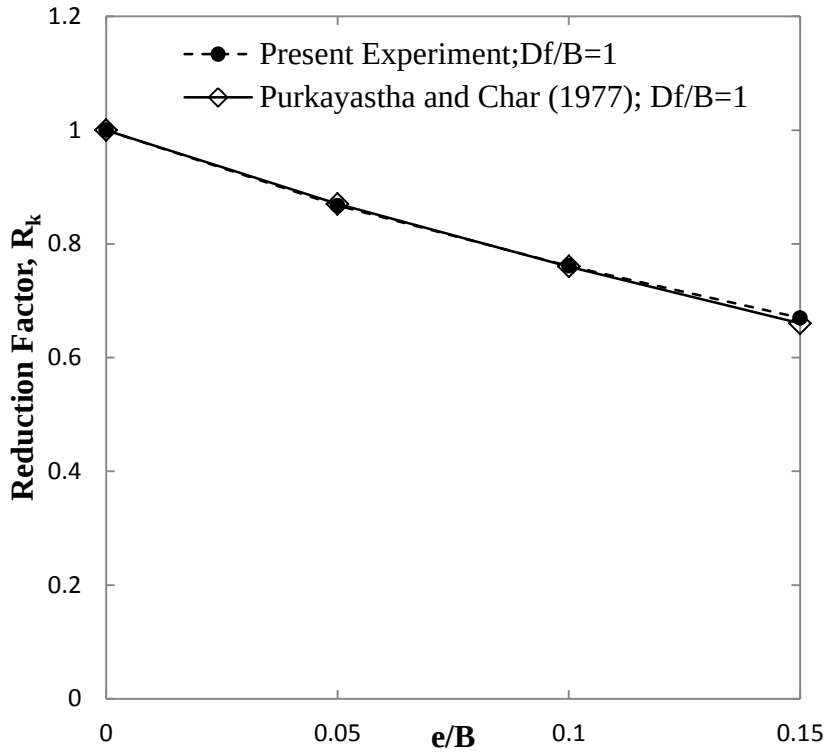

Figure 5.23: Comparison of Present experimental results with Purkayastha and Char (1977) with D_f/B=1

Table 5.8: Calculated values of R_k by Purkayastha and Char (1977) for eccentric vertical condition along with Present experimental values

D_f/B	e/B	Present Experiment; R_k	Purkayastha and Char (1977); R_k
0	0	1	1
	0.05	0.84	0.79
	0.1	0.64	0.65
	0.15	0.54	0.53
0.5	0	1	1
	0.05	0.83	0.84
	0.1	0.74	0.72
	0.15	0.60	0.62
1	0	1.00	1
	0.05	0.87	0.87
	0.1	0.76	0.76
	0.15	0.67	0.66

5.4 Analysis of Test Results

The ultimate bearing capacities of square foundations determined from experimental model tests in the laboratory are given in Table 5.9 (Col. 3). As discussed in section 5.1, in order to quantify certain parameters like *e/B, D_f /B* all the model test results have been analyzed using Nonlinear Regression Analysis (NLREG). NLREG performs statistical regression analysis to estimate the values of parameters for linear, multivariate, polynomial, logistic, exponential, and general nonlinear functions. The regression analysis determines the values of the coefficients that cause the function to best fit the observed data that is being provided. The reduction factor concept as discussed in section 5.1 use the proposed Eqs. 5.2 and 5.3 to predict the ultimate bearing capacity of square foundation subjected to eccentric load. The following procedure is adopted to analyze the test results and develop the reduction factor.

Step 1:

$$RF = 1 - b\left(\frac{e}{B}\right)^n \tag{5.4}$$

for a given D_f /*B* regression analyses is performed to obtain the magnitudes of *b* and *n*. Regression analysis has been done to determine the values of *b* and *n* for each depth of embedment (D_f).

Step 2:

The values of *b* and *n* obtained from analyses in step 1 are shown in Table 5.10. It can be seen from Table 5.9 that the variations of *b* and *n* with D_f /*B* are very minimal. The average values of *b* and *n are* 1.954 and 0.84 respectively. We can assume without loss of much accuracy

$$b \approx 2 \tag{5.5}$$

$$n \approx .8 \tag{5.6}$$

The experimental values of *RF* defined by Eq. (5.2) are shown in Col. 4 of Table 5.9. For comparison purposes, the predicted values of the reduction factor *RF* obtained using Eqs. (5.4), (5.5) and (5.6) are shown in Col. 5 of Table 5.9. The deviations of the predicted values of *RF* from those obtained experimentally are shown in Col. 6 of Table 5.9. It is seen in most cases the deviations are ±10% or less; except in one case where the deviation is about 20%. Thus Eqs. (5.4), (5.5) and (5.6) provide a reasonable good and simple approximation to estimate the ultimate bearing capacity of square foundations ($0 \leq D_f/B \leq 1$) subjected to eccentric loading.

$$q_{u(e/B\ ,D_f/B)} = q_{u(e/B=0,D_f/B)}\left[1 - 2\left(\frac{e}{B}\right)^{0.8}\right] \tag{5.7}$$

Table 5.9: Model test results

D_f/B (1)	e/B (2)	Experimental q_u (kN/m^2) (3)	Experimental RF=$\frac{q_{u\left(\frac{e}{B},\frac{D_f}{B}\right)}}{q_{u\left(\frac{e}{B}=0,\frac{D_f}{B}\right)}}$ (4)	Predicted RF [Eqs.5.4, 5.5,and 5.6] (5)	Deviation $\frac{\text{Col.5-col.4}}{\text{Col.5}}$ (%) (6)
0	0	121	1	1	0
	0.05	102	0.84	0.82	-3.06
	0.1	78	0.64	0.68	5.62
	0.15	67	0.55	0.56	1.40
0.5	0	238	1	1.00	0.00
	0.05	198	0.83	0.82	-1.71
	0.1	176	0.74	0.68	-8.27
	0.15	143	0.60	0.56	-6.99
1	0	339	1.00	1.00	0.00
	0.05	294	0.87	0.82	-6.03
	0.1	258	0.76	0.68	-11.43
	0.15	227	0.67	0.56	-19.24

Table 5.10: Variation of *b* and *n* [Eq. (5.4)] along with R^2 values

D_f/B	*b*	*n*	R^2
0	2.354	0.8558	0.9863
0.5	1.888	0.8297	0.9927
1	1.62	0.8357	0.9996

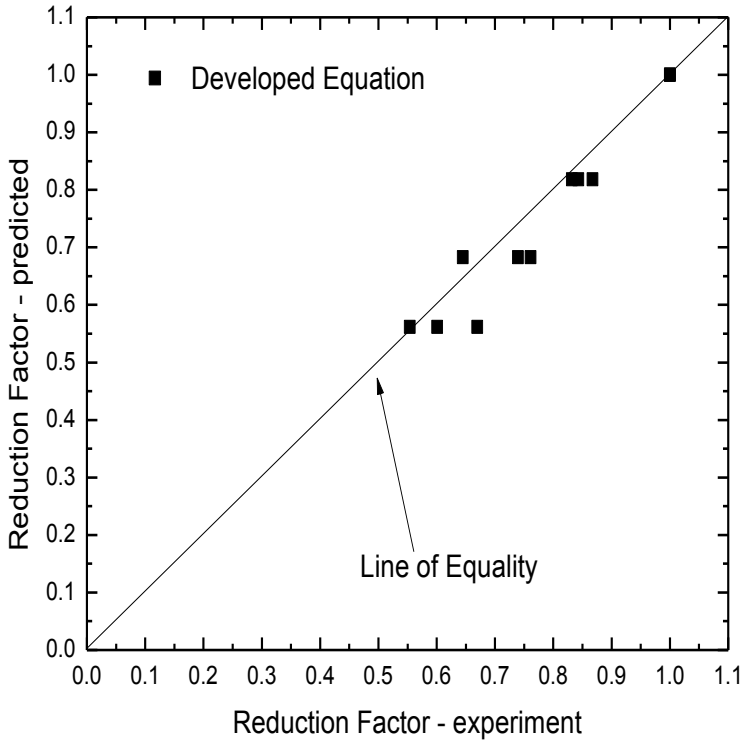

Figure 5.24: Comparison of Reduction Factors obtained from present experimental results with developed empirical Equation

5.5 Comparison

The Reduction Factor is found out from different theories are compared with Present experiment. The developed reduction factor is in good agreement with the theories given by Meyerhof (1953) and Purkayastha and Char(1977). The values obtained are presented in Table 5.11.

Table 5.11: Comparison of Reduction Factor by different theories with Present Experiment

D_f/B	e/B	***RF*** (Experiment) [Eq.5.2]	***RF*** Predicted	***RF*** (Meyerhof)	***RF*** (Purkayastha & Char)
0	0	1	1	1	1
	0.05	0.84	0.82	0.87	0.79
	0.1	0.64	0.68	0.75	0.65
	0.15	0.55	0.56	0.63	0.53
0.5	0	1	1.00	1.00	1
	0.05	0.83	0.82	0.92	0.84
	0.1	0.74	0.68	0.84	0.72
	0.15	0.60	0.56	0.77	0.62
1	0	1.00	1.00	1.00	1
	0.05	0.87	0.82	0.95	0.87
	0.1	0.76	0.68	0.89	0.76
	0.15	0.67	0.56	0.85	0.66

5.5.1 Comparison with Meyerhof [1953]

The ultimate bearing capacity of square foundations at certain depth of embedment subjected to eccentric load on granular soil proposed by Meyerhof (1953) is

$$q_u = qN_q s_q d_q + \frac{1}{2}\gamma B N_\gamma s_\gamma d_\gamma \tag{5.8}$$

To compute ultimate bearing capacity of square embedded foundation, Meyerhof (1963) incorporated *B*' as the effective width in the equation

$$RF = \frac{q_{u\left(e/B\,,D_f/B\right)}}{q_{u\left(e/B=0,D_f/B\right)}} \tag{5.9}$$

At φ=40.8°, $q_{u(centric)}$ and $q_{u(eccentric)}$ at varying depth of embedment (D_f/B=0, 0.5, 1.0) and at eccentricities (e/B=0, 0.05, 0.1, 0.15) calculated for the *RF* from experimental as well as by Meyerhof's effective width theory. This has been shown in Table 5.12. If the average value

of *RF* by Meyerhof's effective width found over the depth at any eccentricity given by table are considered and compared with the predicted values using (b=2, n=0.8),the maximum deviation will be 10 %.

Table 5.12: Reduction Factor Comparison of Meyerhof (1953) with Present results

D_f/B	e/B	Experimental q_u (kN/m^2)	Experimental RF=$\frac{q_{u\left(\frac{e}{B},\frac{D_f}{B}\right)}}{q_{u\left(\frac{e}{B}=0,\frac{D_f}{B}\right)}}$	Predicted RF [Eqs.5.4, 5.5,and 5.6]	RF corresponding to Meyerhof	Deviation $\frac{\text{Col.5-col.4}}{\text{Col.5}}$ (%)
(1)	(2)	(3)	(4)	(5)	(6)	(7)
0	0	121	1	1	1	0
	0.05	102	0.84	0.82	0.85	3.54
	0.1	78	0.64	0.68	0.73	6.52
	0.15	67	0.55	0.56	0.62	9.96
0.5	0	238	1	1.00	1.00	0
	0.05	198	0.83	0.82	0.85	3.54
	0.1	176	0.74	0.68	0.73	6.52
	0.15	143	0.60	0.56	0.62	9.96
1	0	339	1.00	1.00	1.00	0
	0.05	294	0.87	0.82	0.85	3.54
	0.1	258	0.76	0.68	0.73	6.52
	0.15	227	0.67	0.56	0.62	9.96

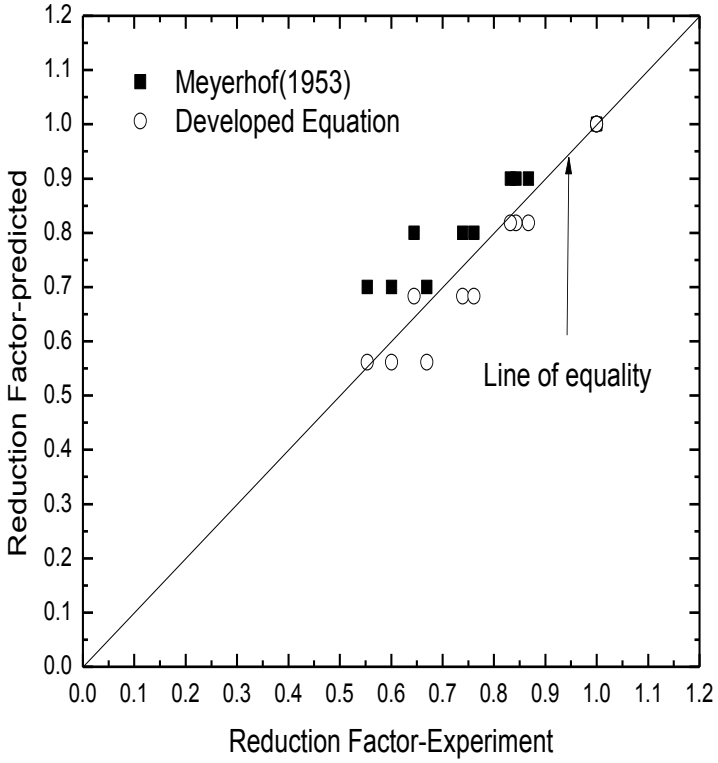

Figure 5.25: Comparison of Present results with Meyerhof (1953)

5.6 Conclusions

The results of laboratory model tests conducted to determine the ultimate bearing capacity of a square foundation supported by sand and subjected to an eccentric load with an embedment ratio (D_f/B) varying from zero to one have been reported. The load eccentricity ratio e/B is varied from 0 to 0.15.Based on the test results and within the range of parameters studied, following conclusions are drawn:

- An empirical relationship for reduction factor in predicting ultimate bearing capacity has been proposed for embedded square footing under eccentric load.
- A comparison between the reduction factors obtained from the empirical relationships and those obtained from experiments shows, in most cases the deviations are ±10% or less; except in one case, the deviation is about 20%.
- The developed reduction factor is in good agreement with the theory given by Meyerhof (1953).

CHAPTER VI

CONCLUSIONS AND SCOPE FOR FUTURE RESEARCH WORK

6.1 Conclusions

- A neural network model equation is developed for prediction of settlement of strip footing in eccentric condition based on the trained weights of the ANN from the existing data set.

$$RF=0.5*(RF_n+1)*(1.635-0.524)+0.524$$

- Load tests have been conducted in the laboratory for embedded square footing (10cm x 10cm) under eccentric load.

- From the present experimental results, an empirical equation has been developed for reduction factor in predicting q_u for eccentric loading condition.

$$q_{u(e/B\ ,D_f/B)} = q_{u(e/B=0,D_f/B)}\left[1-2\left(\frac{e}{B}\right)^{0.8}\right]$$

- The ultimate bearing capacity by reduction factor developed from present experiments is in well agreement with existing theory by Meyerhof.

- The Ultimate bearing capacity for Rectangular footing is more than square footing in surface condition.

- For the eccentric loaded square footing the Bearing Capacity increases with increase in embedment.

6.2 Future research work

The present thesis pertains to the study on the bearing capacity of eccentrically loaded square footing at different depth of embedment i.e. D_f/B=0, 0.5, 1.0 on sand bed and eccentrically loaded rectangular footing (10cm X 20cm) at surface condition. Due to time constraint all other aspects related to shallow foundations could not be studied. The future research work should address the below mentioned points:

- The present work can be extended to study the behavior of rectangular foundations of different sizes at different depth of embedment (D_f/B=0.5, 1.0)
- Large scale study should be carried out to validate the present developed equations.
- The present work can be extended to foundations on cohesive soil.
- The present work can be extended to reinforced soil condition for different depth of embedment.

CHAPTER VI

REFERENCES

Akbas, S. O. and Kulhawy, F. H. Axial compression of footings in cohesionless soils. II: bearing capacity, Journal Geotech. Geoenviron. Eng. 135, 11(2009): pp. 1575–1582.

Balla, A. Bearing capacity of foundations, Journal Soil Mech. and Found. Div., ASCE, 88 (1962), 13-34.

Bowles, J. E., Foundation analysis and design. Mc Graw Hill, 1988.

Briaud, J.L. and Jeanjean, P. Load settlement curve method for spread footings on sand, Proc. of Settlement ’94, Vertical and Horizontal Deformations of Foundations and Embankments, ASCE, no. 2 (1994): pp. 1774-1804.

Briaud, J. L. Spread footings in sand: Load settlement curve approach. J. Geotech. Geoenviron. Eng. 133, no.8 (2007): pp. 905–920.

Cerato, Amy B., and Alan J. L. "Scale effects of shallow foundation bearing capacity on granular material. Journal of Geotechnical and Geoenvironmental Engineering 133, no. 10 (2007): 1192-1202.

Cichy, W., Dembicki, E., Odrobinski, W., Tejchman, A., and Zadroga, B. Bearing capacity of subsoil under shallow foundations: study and model tests. Scientific Books of Gdansk Technical University, Civil Engineering 22(1978): pp. 1-214.

Das, S.K., and Basudhar, P.K. Undrained lateral load capacity of piles in clay using artificial neural network, Comp. and Geotech. 33, no. 8 (2006): pp. 454–459.

Das, B. M., Shallow Foundation Bearing Capacity and Foundation. Second Edition. India, CRC press, 2009.

DeBeer, E.E., Martens, A. A method of computation of an upper limit for the influence of heterogeneity of sand layers in the settlements of bridges, Proc. of 4th ICSMFE, London, U.K., Vol. 1 (1957): pp. 275–282.

DeBeer, E.E.Bearing capacity and settlement of shallow foundations on sand. Proceedings, Symposium on Bearing Capacity and Settlement of Foundations, Duke University, pp. 15-33.1565.

DeBeer, E.E. Experimental determination of the shape factors and the bearing capacity factors of sand, Geotechnique 20, no.4 (1970): pp. 387-411.

Garson, G.D. Interpreting neural-network connection weights. Artif. Intell. Expert 6, no.4 (1991): pp. 47–51.

Goh, A. T. C. Nonlinear modeling in geotechnical engineering using neural networks, Australian Civil Engineering Transactions 36, no.4 (1994a): pp. 293-297.

Goh, A. T., Kulhawy, F. H., and Chua, C. G. Bayesian neural network analysis of undrained side resistance of drilled shafts, Journal of Geotechnical and Geoenvironmental Engineering 131, no.1(2005): pp. 84-93.

Hansen, J. B. A revised and extended formula for bearing capacity. (1970).

Hartikainen, J., and Zadroga, B. Bearing capacity of footings and strip foundations: comparison of model test results with EUROCODE 7, Proc., of 13th ICSMFE, New Delhi, India, Vol.2 (1994): pp. 457-460.

Ingra, T.S., and Baecher, G.B. Uncertainty in bearing capacity of sands, Journal Geotech. Eng. 109, no.7 (1983): pp. 899-914.

IS 6403. Indian Standard for determination of bearing capacity of shallow foundations, code of practice, Bureau of Indian Standards, New Delhi 1981.

Janbu, N. Earth pressures and bearing capacity calculations by generalized procedure of slices, Proc. of 4th Int. Conf. on Soil Mech, and Found. Eng., London, Vol. 2 (1957): pp. 207-211.

Krabbenhoft, S., Damkilde, L. and Krabbenhoft, K. Lower-bound calculations of the bearing capacity of eccentrically loaded footings in cohesionless soil, Can. Geotech. Journal 49, no. 3 (2012): pp. 298–310.

Lundgren, H. and K. Mortensen. Determination by the theory of plasticity of the bearing capacity of continuous footings on sand, Proc. of 3rd Intl. Conf. Mech. Found. Eng., Zurich, Switzerland, Vol. 1 (1953): pp. 409.

Mahiyar, H. & Patel, A. N. Analysis of angle shaped footing under eccentric loading, journal of geotechnical and geoenvironmental engineering 126, no.12 (2000): pp. 1151-1156.

Meyerhof, G.G. The ultimate bearing capacity of foundations, Geotechnique 2, no.4 (1951): pp. 301-332.

Meyerhof G.G. et al. The Bearing Capacity of Foundations under Eccentric and Inclined Loads, In Proc. 3rd Int. Conf. Soil Mech. Zurich, vol. 1, pp. 440-45. 1953.

Meyerhof, G.G. Some recent research on the bearing capacity of foundations, Canadian Geotechnical Journal 1, no. 1(1963): pp.16-26.

Meyerhof, G.G. Shallow foundations, Journal Soil Mech. Found. Div., ASCE 91, no. Proc. Paper 4275 (1965): pp. 21-31.

Michalowski, R.L. & You, L. Effective width rule in calculations of bearing capacity of shallow footings, Computers and Geotechnics 23, no.4 (1998): pp. 237-253.

Olden, J.D., Joy, M.K., and Death, R.G. An accurate comparison of methods for quantifying variable importance in artificial neural networks using simulated data, Eco. Model. 178, no.3 (2004): pp. 389-397.

Patra, C.R., Behera, R.N., Sivakugan, N., Das, B.M. Ultimate bearing capacity of shallow strip foundation under eccentrically inclined load: part I, International Journal of Geotechnical Engineering 6, no.3 (2012a): pp. 343-352.

Patra, C.R., Behera, R.N., Sivakugan, N., Das, B.M. Estimation of average settlement of shallow strip foundation on granular soil under eccentric loading, International Journal of Geotechnical Engineering 7,no.2 (2013): 218-222.

Prakash, S. and Saran, S. Bearing capacity of eccentrically loaded footings, Journal Soil Mech. and Found Div., ASCE, 97(1971): pp. 95–118.

Purkayastha, R. D. Investigations of footing under eccentric loads, Journal Indian Geotech. 9, New Delhi, no.3 (1979): pp. 220–234.

Ranjan, G., and Rao, A. S. R. Basic and applied soil mechanics. New Age International, 2000.

Reissner, H. Zum erddruckproblem, Proc. of 1st Int. Cong. of Appl. Mech., (1924): pp. 295-311.

Saran, S. and Agarwal, R.K. Bearing capacity of eccentrically obliquely loaded foundation, Journal Geotech. Eng., ASCE 117, no. 11 (1991): pp. 1669-1690.

Schmertmann, J.H. Static cone to compute static settlement over sand, Journal Soil Mech. Found. Div., ASCE 96, no. 3 (1970): pp. 1011-1043.

Schultze, E., and Sherif, G. Prediction of settlements from evaluated settlement observations for sand, Proc. of 8th Int. Conf. on Soil Mech. and Found. Eng.1, no. 3 (1973): pp. 225–230.

Shiraishi, S. Variation in bearing capacity factors of dense sand assessed by model loading tests, Soils and Found.30, no.1 (1990): pp, 17-26.

Trautmann, C.H. and Kulhawy, F.H. Uplift load-displacement behavior of spread foundations, Journal of Geotech. Eng., ASCE 114, no.2 (1988): pp. 168-183.

Vesic, A.S., Bearing capacity of Shallow foundations. In Geotechnical Engineering Handbook. Edited by Braja M. Das, Chapter 3, Journal Ross Publishing, Inc., U.S.A, 1975.

Zadroga, B. Bearing capacity of inclined subsoil under a foundation loaded with eccentric and inclined forces: Part 1-method review and own model tests, Archive of Hydroengrg. 22, no. ¾ (1975): pp. 333-336.

Zadroga, B. Bearing capacity of shallow foundations on noncohesive soils. Journal of geotechnical engineering 120, no. 11 (1994): pp. 1991-2008.

Taiebat, H. A. & Carter, J.P. Bearing capacity of strip and circular foundations on undrained clay subjected to eccentric loads, Geotechnique 52, no. 1 (2002): pp. 61–64.

Terzaghi, K., Theoretical soil mechanics. New York, John Wiley, 1943